L3HARRIS: SECONDARY MIRROR SUPPORT STRUCTURE FOR OPTICAL SPACE TELESCOPES

Rachel Anthony **John Luby** **Ognjen Bosić** **Joseph Rodziewicz** **Kadir Sahin**

ABSTRACT

The Secondary Mirror (SM) of an optical space telescope is supported by three struts with ends that attach to the Forward Metering Structure (FMS) of the telescope. Such secondary mirror support structures (SMSS) are found on various satellites, including the James Webb Space Telescope and WorldView-4 Earth remote sensing satellite. Presently, 3D metal printing is not the conventional manufacturing method for satellite applications. For the WorldView-4, graphite composites are used for the mainstream production of satellite parts like the SMSS because of its lightweight and high strength properties. In this project, however, our team explored the practical applications of a 3D metal printed SMSS, designed using a topology optimization tool and structurally analyzed by using the finite element method (FEM). Given a mass goal and loading conditions, the stiffness of the structure was optimized. The rationale behind this research is both economical and geopolitical. The demand for spacecraft is growing each year, which necessitates the need for faster and cheaper manufacturing methods like 3D metal printing. This report reviews the concept generation, finite element analysis (FEA), fabrication, and testing methods involved in constructing an SMSS prototype for our customer, L3Harris Technologies. The resulting design passed all requirements.

PROBLEM DEFINITION

Reflector telescopes are a type of optical telescope assembly (OTA) that often consist of two or more mirrors. The first and largest mirror is the primary mirror (PM), which is a parabolic mirror resting at the back of the telescope. The PM focuses the light onto the SM, a hyperbolic mirror that directs the light onto the detector at the back of the telescope. These mirrors are highly sensitive instruments and unintended displacements of just a few thousandths of an inch can put an image out of focus. Additionally, if the SM is tilted off its intended plane, then a fraction of the captured light will miss the detector. For this reason, it is imperative to have an effective SMSS that ensures a secure SM that has limited movement. Another important characteristic of the SMSS is that it obstructs light from reaching the PM. While a telescope is still functional with the SMSS obstruction, minimizing the shadow of the SMSS onto the PM will increase the intensity of the light that reaches the detector, thus improving the performance of the telescope.

For space telescopes, designing an SMSS requires more design considerations. First, a space telescope likely cannot be repaired if a component fails after launch. As a result, every single component, including the SMSS, is mission-critical. Additionally, during launch, all telescope components are exposed to extreme vibrations, thermal loads, and accelerations. Traditionally, SMSS for space telescopes were manufactured with composites due to their low densities. However, OTA metering structures such as SMSS, are time-consuming and costly to manufacture with traditional manufacturing methods. For these reasons, metal 3D printing has emerged as a potential solution for producing a reliable and relatively inexpensive SMSS.

With a successful metal 3D printed SMSS, manufacturing space telescopes would become faster and cheaper. Once a 3D model is made, it can be manufactured as many times as needed and little extra scrap material is leftover, so there is noticeably less waste. Overall, taking a step towards cheaper space telescopes could help contribute to a future with more operational space telescopes, helping humanity improve its astronomical capabilities.

REQUIREMENTS, SPECIFICATIONS, DELIVERABLES

To ensure the deliverables satisfy the needs of L3Harris, the team worked with the sponsor on creating a list of requirements and specifications for this project. In total, the project has six requirements and nine specifications. All must be satisfied for the project to be considered successful. The requirements are:

1) The project scope is the design, analysis, and prototype of the Secondary Mirror Support Structure only (hosted hardware masses and interfaces are provided for reference and use in finite element models, etc.).

2) L3Harris requests that this project focus on additive manufactured (3D printed) solutions to the problem. L3Harris is currently working on a 3D printed invar (desirable due to low CTE) but invar is not a requirement for this project.

3) The SMSS shall interface to the Forward Metering Structure at three locations 120 degrees apart.

4) The SMSS shall provide interfaces for and support the following hosted hardware (Secondary Mirror and Mounts, Actuator Assembly, Shade Assembly, Misc. Thermal Hardware)

5) Design (CAD model geometry) shall be producible with additive manufacturing methods (3D printing).

6) There shall be no trapped cavities.

The established specifications for this project are:

1) The outer diameter of the SMSS (interface to the FMS) shall be 48 inches.

2) The first mode of the SMSS shall be 120 Hz or greater when grounded at the FMS interface and supporting all hosted hardware.

3) SMSS Mass: The goal is 18lbm.

4) The SMSS shall have positive margins of safety against yield and ultimate failure when exposed to a quasi-static load of 12 G laterally and 18 G axially simultaneously (lateral swept 15º increments) combined with a 5ºC to 35ºC temperature range (Nominal room temperature is 20ºC) while supporting all hosted hardware.

5) The SMSS and hosted hardware shall not obstruct more than 14% of the PM clear aperture area.

6) The structure must be able to support the mass of the 23lbm of hosted hardware (secondary mirror, baffle, actuator plus additional dead weight – not physically shown in CAD model).

7) The following design factors of safety shall be used in the analysis (if applicable):

- Yield: 2.0
- Ultimate: 2.5
- Buckling: 4.0

8) The following mass contingency factors shall be used (if/where applicable):

- Concept design: 20%
- Preliminary design: 15%
- Final Design: 10%
- Post-Final Design: 5%
- Measured hardware: 0.10%

9) The SMSS should provide a stable mounting platform for the Secondary Mirror (SM) in thermal environments. The average motion of the SM interfaces under a 1ºC isothermal load should be 0.66 micro-inches translation (RSS of X and Y) or less and 0.037 micro-radians rotation (RSS of Rx and Ry) or less.

Our team and the sponsor established six deliverables for this project. The team will send these items to the sponsor over the course of the project. Details on the deliverables can be found in the work breakdown structure diagram found in Appendix A. The associated activities for the deliverables can be found in the critical path management diagram found in Appendix B. The deliverables are:

1. CAD file prototypes using NX (step file format) and 2D drawings.
2. Finite Element Model (FEM) in Nastran.
3. Final design report.
4. Host design review meetings and provide supporting slides and drops of the CAD and FEM: Concept Design Review, Preliminary Design Review and Final Design Review.
5. 3D printed prototype (can be scaled and from the material of choice).
6. Reports on any model validation – could be included in the design review and final report.

CONCEPTS

As a part of the concept generation process, each team member created a sketch of one potential design. Based on these sketches, each member created a CAD model in NX and performed an FEA on it. Three FEA load cases were considered: modal analysis, thermal analysis, and launch load analysis. These required inputs of the material, boundary conditions, and applied loads used, which were taken directly from project specifications.

The first mode along with maximum stresses for each of the designs and several other factors are shown in Table 1. These factors were implemented in the Pugh Matrix which was used to determine which designs have the greatest potential. The Pugh Matrix is shown in Table 2.

PDR: Performance of Concepts					
	I	II	III	IV	V
First Mode (Hz)	447	421	231	19.66	299.18
Max thermal stress (psi)	9560	12200	11090	10672	7411.34
Max load stress (psi)	1718	1317	1090	50660	3295.72
Mass (lbf s^2/in)	0.243	0.239	0.306	0.193	0.202
PM Shadow (%)	14.9	13.3	7.61	13.5	16.5

Table 1: Performance of concepts

I-Beam Cross-Section [I]

The I-beam-shaped support structure was designed to minimize bending. I-beams are known to reduce and resist sheer stress and bending movement. FEA simulations showed that this concept had the highest first mode when grounded at the FMS interface. This design also sustained the highest maximum thermal stress of all the concepts. [Appendix C].

Solid Center Structure [II]

The solid center structure was designed with the idea to make the diameter of the center smaller and the legs as skinny as possible, thus maximizing the percentage of light passing

through. The height requirement for this structure ended up being significantly lower than for the WorldView-4 telescope, so the concept was scrapped. In terms of FEA simulations, this structure had the second-highest first mode. While neither the mass nor the highest stress experienced ranked as the best, the strength/mass ratio was the best of all structures. [Appendix D]

Double Rod Structure [III]

The absence of curvature allows for less material. The double rod feature thickens the shape of the overall support and could improve the stiffness of the structure. Simulation from FEA showed that this concept sustained the greatest maximum thermal stress out of all the designs. This concept also had the most favorable PM shadow obstruction. [Appendix E].

Tapered Support Legs [IV]

This concept features a support structure with tapered titanium legs. Like the Solid Center Structure, material was conserved by means of tapering. This concept was designed to consider the weight requirement provided by the sponsor. In theory during modeling stages, incorporating a taper would make it simpler to adjust leg thicknesses to reach the target mass of 18lbm. Out of all the concepts, this design sustained the greatest maximum load stress during FEA simulation but had the lowest first mode when grounded at the FMS interface, which was below the sponsor-required minimum first mode. [Appendix F]

Doughnut Structure [V]

The doughnut concept shown in Appendix G attempts to mimic the design of the secondary mirror support structure shown on the WorldView-4 satellite, shown in Appendix H. The absence of material in the center of the structure intends to minimize the obstruction of light caused by the shadow of the SMSS, while the curved beams were designed to increase the efficiency of the transfer of loads applied due to extreme temperature, gravity, and launch conditions. Despite the design efforts, this design had the greatest PM light obstruction of all the concepts. [Appendix G]

The Pugh matrix is a matrix that allows for objective comparison between several design candidates which ultimately leads to the design that best meets the set of criteria. The criteria on which our team based the matrix are the following: print time, printability, PM shadow, room for optimization, and SMSS arm largest dimension. These 5 criteria were deemed critical when designing our structure. The print time increases the cost of the design, and we were given a budget of only $1,000. The printability of the structure is important in case of overhang. If the overhang angle is too large, the print will not be properly supported, and it will fail. The PM shadow is a requirement that must be under 14% and is a critical requirement to not interfere with the light passing through the PM. The potential for further optimization was also an important consideration when choosing a design because some designs had limited room for changing the structure in the CAD model. Designs that were closest to the maximum allowable stress had the least room for removing material and optimization. Lastly, the final criterion was the SMSS arm largest dimension. This criterion was based on using minimal material for the design. Some designs have different heights and increase the amount of material used. In this criterion having a larger arm is considered wasteful and is not an optimized structure.

The baseline model for the Pugh matrix was the solid center structure since the design passed all requirements. As shown in the figure below, each criterion had a + sign for better than the baseline model, a 0 for about the same as the baseline model, and a – sign for if the design performs worse than the baseline structure.

Pugh Matrix					
	I	II (Base)	III	IV	V
Print Time (Volume)	-	0	-	0	0
Printability (Overhang)	-	0	-	0	0
PM Shadow (<14%)	0	0	+	+	0
Room for Optimization	0	0	+	--	0
SMSS Arm Largest Dimension	-	0	0	-	0
TOTAL	-3	0	0	-2	0

Table 2: Pugh matrix for design concepts

From the Pugh matrix, the most promising designs were the solid center structure, the double rod structure, and the doughnut structure. However, none of these were selected for the final design.

MODEL OPTIMIZATION

Topology optimization is the principal modeling method chosen for the final SMSS design. As such, the Pugh Matrix was not a significantly helpful tool in determining a concept to move forward with since Siemens NX, the primary CAD software used for this project, decided the final geometry mathematically. However, the Pugh Matrix did guide preliminary drawings and the design of an initial STEP file. This STEP file was sent to a third-party 3D metal printing service for our first rough order of magnitude (ROM). Concept V (Doughnut Structure) was selected for the initial 3D metal print ROM process. Due to the similarities between this concept and the WorldView-4 SMSS [Appendix H], it was determined that the geometry of Concept V, pertaining to the specifications required by L3Harris, would provide the most accurate cost estimate.

The ROM received was from an aerospace 3D printing company FAMAero, based in Frankenmuth, Michigan. The 100% scale titanium model was quoted at $45,400 based on the design of Concept V [Appendix G]. Due to the high price of

titanium and invar, designing a lightweight model that used the least amount of metal proved critical, since the 3D printing and treatment processes are costly. Our team decided to move forward with the topology optimization method in our design process, effectively allowing Siemens NX to use its own algorithm to determine the most optimal shape for our structure.

Regarding material selection, titanium 6Al-4V (Ti-64) was chosen. Titanium in general features a much higher yield stress much higher than that of common steels and aluminum. Additionally, titanium is about half as dense as common steels, which is critical because the mass of the SMSS itself is a major contributor to the applied load. Invar was considered, however, the thermal requirements of 15ºC swings from 20ºC were not demanding enough to justify prioritizing a low coefficient of thermal expansion (CTE) over other properties such as yield strength and density.

The result of the topology optimization given the bounding body shown in Appendix K. The team gave the optimizer tool a given set of loads and directions for those loads, as well as boundary conditions. These included the gravitational loads required by the sponsor and fixed constraints that represent the mounts of the structure as explained in the Requirements, Specifications, and Deliverables section. The optimizer's assigned objective was to maximize the stiffness while attaining the target mass of 18lbm and not surpassing 50% of the yield strength of Ti-64. Optimizing for stiffness was chosen because it will increase the first natural frequency, and it will also minimize displacement for the same load. Given the optimized model, the external solid body was expected to perform better during simulations than any of the previously designed concepts. However, the optimizer itself cannot be relied on for producing the most reliable results, as topology optimizers consist of many approximations during calculations, including linear approximations for stiffness equations, and curve-fitting onto voxel-based geometry to produce smooth surfaces. The optimizer could not reach the target mass, as it was limited by the 50% of yield stress requirement. However, this issue was not irreconcilable, as the infill optimization that later occurred cut out more than enough mass to meet the target mass.

While topology optimization provides a solid geometry that maximizes stiffness while targeting a specific mass, it does not change the geometry of the interior. However, a unique characteristic of 3D printing is that it allows for geometry changes on the interior of the structure by implementing various lattice shapes. This can often decrease mass significantly with a small decrease in stiffness. Since every pound launched into space is expensive, interior geometry changes can also help decrease project costs. Therefore, after the SMSS was topologically optimized, lattice was applied to the interior of the structure. To do this, the NX "Lattice Body" tool was used. This process involved loading the optimized structure to NX, applying a specific lattice type to it, loading it to the FEM file, and applying a specific outer thickness in the FEM file. This would result in a shelled structure with a 2D mesh on the outside and a lattice structure with a 1D mesh on the inside which would then be connected with an RBE2 rigid connection.

There are many different lattice types in NX. Based on ease of printing, CAD complexity, stiffnesses in various directions, overall porosity, and time constraints, the team decided to only explore three types of lattice structures available in NX. The use of two other, more complex structures were attempted, but due to the complexity of models generated, simulation times were too long given the time constraints of the project. The following three lattice types were explored: TriDiametral, BiTriangle, and QuadDiametral. All three lattices are self-supporting, as they have overhang angles of 45 degrees or less. This would allow printing with Direct Metal Laser Sintering (DMLS) without support structures for the lattice.

The QuadDiametral lattice type has identical stiffness in the three main planar directions as can be seen in Appendix L, which along with its simplicity, was the main reason why it was selected. Having the same stiffness in the XY, YZ, and XZ planes allows for more flexibility regarding lattice orientation. The other two lattice types are also shown in Appendix L and they both have identical or very similar stiffness in two directions, with the stiffness in the third direction being much higher. Because most of the load applied to the SMSS is in the axial direction, both the TriDiametral and BiTriangle lattices are oriented in such a way that the stiffest direction is the axial direction, while the two lateral directions both have similar, lower stiffness.

As previously mentioned, the FEM model consisted of the lattice applied to the entire body. This does not reflect the actual design of the final model, because the mounting points of the final model will need to have solid infills around them. For mass calculations, this approximation was taken into account by adding the mass of these solid infill areas to the corresponding point mass of each mounting point. Each mounting point is connected to the faces

MECHANICAL ANALYSIS

Some specifications required mechanical analysis. Analysis on this project was conducted through NX NASTRAN software, which involved running two different types of simulations. These simulations were used to determine the first mode of the structure, maximum stresses experienced, maximum displacements and the buckling modes. Data was then compared to the results obtained through testing.

One of the simulations was the modal analysis for which NX Solution 103 Real Eigenvalues was used. This helped the team acquire the modal frequency data and compare it to the desired 120 Hz. For modal simulations, no loads were applied, but boundary conditions were set. This meant that the faces at the ends of the structure were all fixed, but neither gravity nor the thermal loading were applied. This is shown in Appendix M.

The other simulation was the NX Solution 105 Linear Buckling. This simulation allowed the team to understand where areas of high stress and displacement are and their magnitudes. It also provided the buckling modes of the structure. In addition to setting boundary conditions, for the Solution 105 simulations, all loads described in the specifications section were applied.

This included both the gravity load of 21.6G and the thermal load of temperature change from 20 ºC to 35 ºC. Initially, the third simulation with temperature change from 20ºC to 5ºC was also run, but the results were almost identical to the 20-35ºC temperature change. Since 20-35 ºC results were slightly worse in all aspects, the team decided to save time by only considering one of the thermal loads. The finite element model for the simulation is shown in Appendix M.

The results of these simulations were critical to determine the best lattice type and the optimum shell thickness. Therefore, an optimization model log was used to track the results of all simulations conducted by the team. Shell thicknesses between 0.02 and 0.15 inches were considered and combined with the three lattice types. Each simulation took about one hour to complete, so to save time not all modal analyses were conducted. Data obtained through all the simulations is shown in Appendix MM.

The QuadDiametral lattice-type performed better than all the other lattice types in terms of the first mode of frequency, maximum stress, buckling mode, and maximum displacement. It had a slightly higher mass due to having lower porosity, but the team believes that the difference in performance can help with decreasing the shell thickness which can improve the mass of the QuadDiametral structure.

Tolerance Analysis

Another mechanical analysis that our team performed was two interference test fits. Our design will be fully constrained at the mounting legs, so the team decided to press-fit plastic dowels into the aluminum support legs to hold down the structure when testing the design on the Newport table. The plastic dowels have a diameter of approximately ¼ of an inch. A magnetic Newport table is used to stabilize and support items during testing. After receiving advice from Professor Muir, our team decided to tolerance the fit in increments of 0.001 inches from the ¼ inch diameter, so that the diameters that were tested were around +0.003 to -0.002 from 0.25 inches. Our team 3D printed 6 different blocks each containing 5 of the same sized holes to be tested. 5 of the same size holes were printed since the tolerancing on a 3D printer is not perfect and could be inaccurate sometimes. The appropriate fit for a dowel is when the hole's diameter is 0.253 inches. The plastic dowel was able to snugly fit into the plastic blocks. The image of how the plastic dowels fit into the test blocks is shown in Appendix R.

The team also performed a mechanical analysis on the inserts that needed to be heated into the support. The purpose of these inserts was to connect the loading plate to the SMSS and conduct tests. A similar process was used for the plastic dowels, where multiple blocks with varying hole sizes were printed. With a soldering iron, our team heated the insert over the soldering pen and gently pushed the insert into the plastic blocks that our team printed. The best tested fit was 0.23 inches for the insert and 0.26 inches for the bolt. The fit of the heated insert into the test block can be seen in Appendix R.

Our team later found an alternative using soldering iron-heated inserts in our SMSS prototype. Our team decided to obtain longer screws and hung the load plate from the SM mounting points by using threaded nuts. This approach was taken because inserting heated threaded inserts would be more complicated and would introduce new risks into the test setup, including the risk that all inserts would need to be installed perpendicularly to the face plane of the mount.

Further tolerance analysis of the scaled printed prototype was performed. First, each of the printed thru-holes was measured with calipers. The holes are labeled in Appendix T. The results of these measurements and their corresponding CAD dimensions are shown in table 3.

Hole	CAD Size (in)	Measured Size (in)
A (top)	0.251	0.252
A (bottom)	0.251	0.251
B (top)	0.251	0.252
B (bottom)	0.251	0.2525
C (top)	0.251	0.2515
C (bottom)	0.251	0.2525
D	0.26	0.259
E	0.26	0.2595
F	0.26	0.26
G	0.26	0.26
H	0.26	0.2595
I	0.26	0.26

Table 3: Measured hole diameters for printed holes in 60% scaled prototype.

All measured hole diameters fit the tolerance of -0.0005, +0.0015. This tolerance could be insufficient for press-fit connections, which require a lower tolerance of zero.

Furthermore, the overall size of the printed prototype was measured using a FaroArm, a coordinate measuring machine (CMM) shown in Appendix S. The FaroArm measured the flatness of four planes. Referring to Figure [xx], the plane containing holes D-I had a flatness of 0.001929". The flatness of the planes at the end of legs A, B, and C, respectively, are 0.001212", 0.002362", and 0.001299". Flatness tolerances are especially important for the faces on the ends of the legs, where an uneven face will result in uneven load distribution across the face and induce localized contact stresses. However, the end mounts of the legs are solid Ti-64, and these localized contact stress points are unlikely to cause deformation that would compromise the function of the SMSS.

Additionally, the distance between the top leg hole and the midpoint of the two nearest SM holes was measured with the FaroArm. In the 60% scaled CAD model, this distance was measured as 11.7205". For legs A, B, and C, respectively, this

distance was measured to be 12.0695", 12.0637", and 12.0709". Of all measured dimensions, this dimension was the largest and varied the greatest from the target length. The greatest deviation from 11.7205" was found on leg C, which was longer by 0.3504". Variation this large could threaten the functionality of a full-scale printed structure. However, a laser-sintered titanium prototype would not face the same tolerance issues that an FDM-printed plastic prototype does. In general, metal laser sintering printers are much more accurate than FDM plastic printers. A redeeming quality of these loose tolerances is that they could potentially be saved with traditional subtractive manufacturing methods post-print.

Lattice Testing

To understand the mechanical properties of different lattice structures, our team created 6 5-inch blocks with the approximate thickness of 0.5 inches and width of 0.7 inches. To test which lattice structure performs best, a bending test was conducted. The standard procedure is to secure a block at an equal and set distance away from the cylindrical supports. The bending test was conducted at the Mechanical Engineering building using an MTS (Material Test System) machine. Appendix V The flexure fixture was attached to the machine and the extensometer to read the displacement of the lattice block. The flexure fixture places increasing weight to the structure, the MTS machine recorded the force and the displacement of the block, and the data was recorded and analyzed. From the data, the stiffness of the lattice structure can be obtained by the equation:

$$k = \frac{F}{\delta} \quad (1)$$

where k represents the stiffness, F is the force applied to the block, and δ represents the displacement. The data was then put in the graph shown in Appendix W.

From this data, our team was able to find out that the third sample had the highest stiffness, which was the QuadDiametral lattice structure at a 30-degree angle. Data on the length, width, and thickness of each block was measured using calipers and can be found in the table below.

Specimen	Length	Thickness	Width
Sample 1	5.017	0.507	0.705
Sample 2	5.019	0.504	0.708
Sample 3	5.018	0.508	0.708
Sample 4	5.021	0.505	0.707
Sample 5	5.023	0.504	0.707
Sample 6	5.025	0.505	0.709
All numbers are in inches			

Table 4: Recorded measurements of blocks with a lattice structure

In addition, the lattice structures are in Appendix X which shows the printed blocks vs. the CAD model of the blocks.

MANUFACTURING

We planned for our original model to be 3D metal printed out of Titanium. After conversing with FAMAero, it became apparent that there were not enough funds to print a full model or even a scaled-down model. The team discussed and decided that there was no physical way to print a metal model with the funds given, it was decided that 3D printing a model in ABS-M30 would be more realistic given our budget constraint. Our model is required to be 48 inches in diameter. The final print model was printed at 60% of its original size at 28.8 inches in diameter, so the printer could print the whole part at once. From the time we submitted our model to be printed to the time we got it was about a week. The total model costs approximately $450 with a $150-$200 express shipping cost. The 60% reduced model can be viewed in Appendix EE. The drawing of the 60% reduced model can be seen in Appendix FF.

Before printing our 60% percent model, our team also printed a 20% scaled-down version of the design to be printed. The printed 20% model showed the printability of our finalized structure at a small scale. The time it took to print the 3D model was around 2 hours, when printed with FDM on a Stratasys F270. Appendix GG.

For the mounting to connect to our team's design we had to produce a way to properly constrain the design. Our team focused on using fasteners or hinges but decided to use a press fit to secure the mounting plate to the design. Our team ordered plastic dowels and tested the fit as stated in the mechanical analysis section. The plastic dowels cost about $5 for 25 pins.

To analyze how well the pin fit, our team decided to print out 6 different blocks with 5 of the same sized holes. It took approximately 20 minutes to print three blocks. Therefore, the print time was about 40 minutes to create these test blocks. The cost of the interference fit test cost about $67 to manufacture the pin test blocks.

During the tolerance analysis of the inserts and bolts, 6 plastic test blocks were created for testing the insert and 4 plastic test blocks were created to test the bolts. This is an additional 10 testing blocks that were printed. It takes about 8 minutes to print out each small test block. The approximate cost of printing the ten small test blocks would be $134.

In the process of starting our manufacturing of the 3D printed mounting legs, our team thought it would be acceptable to create plastic support mounts because our final deliverable is plastic and not titanium. If our team wanted to thoroughly test our design, metal supports are incomparably stiff compared to the plastic design. Therefore, our team switched our focus from plastic supports to metal supports. The metal aluminum supports will more accurately represent the real-life constraint conditions of this project. With the base of the supports being so thin, 0.15 inches, there was concern that a plastic model would deform.

To create the metal supports, our team used an L-shaped aluminum block and used the bandsaw to cut out 3 support

brackets. The picture of the 3 support legs before the bandsaw cut the L-shape block is in Appendix HH. These blocks were then cut once more to the drawing specifications. The drawing specifications can be seen in Appendix II.

The finished design of our support legs has two holes, one of which is unforgiving in the height placement of the top hole, while the second hole is a slide fit which is more forgiving when machining. The holes were created using a 3-axis Bridgeport-style vertical milling machine. Moreover, the bottom surface of the support was then cut through the middle to create an opening for the magnet to properly lay on and constrain the metal supports to the Newport table. After trimming the excess material off, the supports were then sanded and smoothed from the belt sander and file. The milling process and final mounting legs can be seen in Appendix U.

The cost of machining these mounting legs would have cost about $1000 if the price for manufacturing cost was $100/hr. The production drawing of the mounting legs can be seen in Appendix II.

For the load plate that will be attached to our design, our team decided to make the material out of plastic because the material will not affect the testing conditions. The only difference between using a metal mounting plate and a plastic mounting plate would be the difference in weight of the material and the time it would take to manufacture. Therefore, our team printed out the mounting plate with the same size holes as discovered in the tolerance analysis. The load plate is located in Appendix JJ.

As shown in the figure above, the screws fit in the mounting plate and were screwed into the SMSS. Screws, nuts, and watchers were purchased for less than $10. Also, the inserts were soldered into the design of the SMSS and connected the support to the mounting plate. The printing time for the load plate took about 4.5 hours. With the assumption that print time is $100/hour, the cost of this load plate would be $450.

In addition, there were 6 different blocks containing three different lattice structures; then 3 more blocks of the same three lattice structures but angled at 30º. The blocks were printed to test for bending. The approximate time it took to print the lattice blocks was 10 hours, excluding 4 hours of dissolving the support structures inside the block. The cost of printing 6 lattice blocks is estimated to cost $1,000.

When considering the team's hours working on this project. The same assumption is applied which is that it cost about $100/hour to work on this project. Our team utilized scrum hours to record the amount of time we put into this project. The total cost as a team and per person is shown in Table 10. These times represent the amount of time taken for this project which includes, but not limited to, creating CAD models, doing simulations, testing etc.

First	Total Hours Worked	Cost ($100/Hr.)
Rachel Anthony	145.5	$14,550.00
Ognjen Bosic	137	$13,700.00
John Luby	176.5	$17,650.00
Joseph Rodziewicz	161	$16,100.00
Kadir Sahin	146.5	$14,650.00
Total	766.5	$76,650.00

Table 10: SCRUM hours

	Cost
3D Printing	
20% Reduced Model	$200.00
60% Reduced Model	$600.00
Load Plate	$450.00
Pin Testing Block	$67.00
Insert and Bolt Test Block	$134.00
Lattice Blocks	$1,000.00
Plastic Dowels	$5.00
Machine Time	$0
Mounting Legs	$1,000.00
Team's Total Cost ($100/Hr.)	$76,650.00
Total Cost of Project	$80,106.00

Table 11: Total cost of project

The total cost of the entire project is about $80,106.00 as shown in the table above. The entire project is extremely expensive to manufacture a singular part. Some changes that could potentially reduce the cost and build time would utilize the lattice structure of the internal system. Including a lattice decreases the amount of material used and would decrease the cost of production.

TEST PLAN AND RESULTS

A displacement test was conducted on the 60% scaled model. To understand the stiffness and structural properties of our final printed design, our group placed our SMSS structure on a Newport table. The structure was supported by aluminum mounting legs and a magnet at each end of the mounting legs. The displacement of the model was recorded with a height gauge.

For the vertical displacement test, the height gauge was placed directly above the SMSS at a point between two SM mount holes. To attach weight to the structure, the loading plate

was hung loosely with six M5 bolts with threaded nuts. The loads added to the plate were from a hook weight set in kilograms and then later the weight was converted into pound-force. The height gauge was set at an initial reading and the difference after the weight was added to the system was the vertical displacement of the structure. This was recorded for each leg with increasing mass. The tables below show the vertical displacement of the structure at each leg when a mass is applied. From this test, the force over displacement results correspond to the SMSS's overall stiffness in the direction of the load when applied at the center point of the structure.

Leg A		
Initial Height Gauge Reading	0.163 inches	
Pound-Force	Reading (Inches)	Displacement (Inches)
0.440925	0.1595	0.0035
1.10231	0.155	0.008
2.20462	0.149	0.014

Table 5: Vertical displacement of Leg A

Leg B		
Initial Height Gauge Reading	0.1635 inches	
Pound-Force	Reading (Inches)	Displacement (Inches)
0.440925	0.1595	0.004
1.10231	0.154	0.0095
2.20462	0.15	0.0135

Table 6: Vertical displacement of Leg B

Leg C		
Initial Height Gauge Reading	0.137 inches	
Pound-Force	Reading (Inches)	Displacement (Inches)
0.440925	0.1325	0.0045
1.10231	0.128	0.009
2.20462	0.1242	0.0128

Table 7: Vertical displacement of Leg C

The second part of the displacement test was the horizontal displacement. The configuration of this test differed from the vertical test in that the mass was redirected with a block and the height gauge was placed horizontally between the SMSS's legs. The block acted like a pulley system and changed the direction of the force, which is how a force can act horizontally on the system. Initial measurements were recorded, and the measurements are shown in the tables below. Moreover, images of both test set-ups are shown in Appendix Z for the displacement test.

Between Legs A & B		
Initial Height Gauge Reading	0.059 inches	
Pound-Force	Reading (Inches)	Displacement (Inches)
1.10231	0.0595	0.0005
2.20462	0.06	0.001
3.30693	0.0605	0.0015

Table 8: Horizontal displacement between Legs A & B

Between Legs B & C		
Initial Height Gauge Reading	0.0895 inches	
Pound-Force	Reading (Inches)	Displacement (Inches)
1.10231	0.09	0.0005
2.20462	0.0905	0.001
3.30693	0.0915	0.002

Table 9: Horizontal displacement between Legs B & C

A modal strike test was conducted by the team to measure the first mode of frequency of the 60% scaled structure. Appendix CC depicts the setup of the accelerometer on the moving mass of the vibrating body, which captured the first mode of vibration in the vertical direction. The accelerometer was attached toward the center of the structure using beeswax as an adhesive. Before testing began, the data acquisition software was calibrated using a stroboscope. The modal test results for the scaled model found a natural frequency of 66 Hz, which was substantially lower than the expected result of 140 Hz based on the simulations of the same 60% model. The modal test result data is shown in Appendix DD.

Results

Specifications 1 and 3 can be measured using dimensioning tools in NX. The diameter was set to its required length, and the physical model does not meet the requirements, only because it was scaled down. The mass on NX does not meet the weight requirement of 23lbm until the lattice is applied. Once the lattice was applied, the mass was cut down to approximately 9lbm.

Specifications 2 was measured with NASTRAN modal simulations. The final model met the requirement, however different lattices and different 2D mesh sizes can change the natural frequency, as can been seen in Appendix MM.

Because it's virtually impossible to test the quasi-static loads listed in Specification 4, NASTRAN was used to test the model on the computer, and then a simple displacement test was used on our physical model. For our physical model, a load plate (see Appendix JJ) was designed to connect to our model. It was connected through the holes and weights were loaded on it. See Appendix HH for results.

Specification 5 discussed that the SMSS and its hosted hardware, including secondary mirror, actuator assembly and

shade assembly, shall not obstruct more than 14% of the PM clear aperture area where light would pass through. The topology optimized model and the hosted hardware obstructed approximately 12% of the PM. This percentage value was calculated by creating a 2D sketch plane on the top view of the SMSS model in NX, then creating splines surrounding the figure to subtract the enclosed areas from the area of the solid body. The hosted hardware shadow was included in the calculation, while the hole in the PM was not considered in this calculation.

Requirement	Result
1	Satisfied
2	Satisfied
3	Satisfied
4	Satisfied
5	Satisfied
6	Satisfied

Table 12: Fulfillment of the requirements

Specification	Result
1	Satisfied
2	Satisfied
3	Satisfied
4	Satisfied
5	Satisfied
6	Satisfied
7	Satisfied
8	Satisfied
9*	*See Table 14*

Table 13: Fulfillment of the specifications

Numerical Requirement	Full-Scale Simulation Result
Max Stress: 49022 psi	~23000 psi
14% obstruction	~12%
120 Hz	124 Hz
Buckling (SF = 4.0)	30.75
Mass: 18lbm	~9lbm
*Micro Yield: 0.66 µin RSS translation	14.9 µin
*Micro Yield: 0.037 µrad RSS rotation	0.72 µrad

Table 14: Simulation results for full-scale model

INTELLECTUAL PROPERTY

Our design of the SMSS is patentable. The topology optimization tool was used to reduce the excess material to make the structure as efficient as possible. Topology optimizers produce unique geometry that is highly dependent on inputs. This combined with the lattice selection makes our SMSS design un-obvious and novel.

Companies such as Lockheed Martin Company or Boeing company have their own patents for their space telescope's components. The space telescope in Appendix KK is from the Lockheed Martin Company. The Lockheed Martin Company decided to make their SMSS with a series of thin rods to create their structure. Note that each telescope has a unique design, therefore the SMSS from the different telescopes will vary in their design if the telescopes are different.

The Boeing Company's SMSS found in Appendix LL is unlike our design. In our design, we did not give much height to our structure, which mounted to the FMS. Moreover, in our design, our structure's legs are designed to act as cantilever beams. In the Boeing Company design, they focused on a straightforward design using rods. By using NX, the topology optimization application allowed our design to be optimized efficiently [Appendix K]. The topology optimization application tries to minimize the amount of material used while maintaining the design's mechanical stiffness.

Our design was produced mathematically by Siemens NX software which produced a unique and novel solution. Therefore, our design is patentable for its originality.

SOCIETAL AND ENVIRONMENTAL IMPLICATIONS

The use of 3D printing has become popularized due to its quickness over traditional manufacturing methods. 3D metal printing uses much more energy to create a design of the same material and mass than it does to machine the material into the desired design. [3] Requirement 1 prompted us to explore the use of 3D metal printers and their production speed to make an SMSS in a timelier manner.

Environmentally, this project does increase the amount of pollution and energy waste than the typical manufacturing of a part. The carbon footprint per kilogram of material processed is larger in 3D printing than in traditional manufacturing. Additionally, 3D printers typically use plastics that are not biodegradable, which increases plastic waste. [4]

For our project, we utilized plastic printing instead of metal printing. Metal printing can be less wasteful than some traditional manufacturing, but 3D printing has been popularized due to its efficiency and high precision when creating an object. Due to the rise in the popularity of additive manufacturing, there could be problems with increases in energy consumption. [4] Also, from 3D printing, there could be more plastic waste as a result. One positive impact is that there is less wasted material in additive manufacturing. In traditional manufacturing, not all the material is not being fully utilized since the material will be cut and shaped.

Internal lattice structures were optimized in the design to reduce the energy consumption and to reduce the overall print time and material used. Infills are a good way to reduce material and energy consumption in most applications. Not every design

should be a solid print unless it is vital to the design. Topology optimization takes a 3D CAD design and removes material to get the most efficient design. This is how our team reduced the excess mass of the structure while also decreasing the amount of energy being used in the process of creating our SMSS.

A societal impact of 3D printing, commonly referred to as a zero-skill form of manufacturing, is that it puts traditional manufacturers out of work. Since 3D printing can easily be used and it can produce many different products including jewelry, tools, and toys, this would also then slow down the production of those said companies.

Overall, 3D printed SMSS's could cut down on lead times and costs for production of space telescopes. This could help lower the production costs of space telescopes in general and open the market to more potential consumers. This would open more opportunities for advancement in astronomy and satellite imaging in general.

RECOMMENDATIONS FOR FUTURE WORK

If given the opportunity to work on this project for another six months our team would make a few changes. Firstly, we would have printed our design with a lattice instead of a solid infill. Our team experienced many problems with the NX software when meshing the shell and the lattice and the CAD file would not work. With the help of Professor Muir, revised our model and applied a 2D mesh in the FEM to work as a shell, then began simulating different internal lattice structures.

If given more time, our team would test each lattice structure given from NX and our own designed lattices. This also means that we would have approximately 25 different simulations per lattice (24 different applied gravity loads and a modal simulation). This would take over 20 hours of testing per lattice and this is not even considering complex lattice structures. Complex lattice structures are structures that cannot be printed without support structures due to large overhang angles, which would decrease the printability of the design.

A Taguchi design of experiments (DOE) study could also be conducted if there was more time and resources available. The DOE would require the use of several factors, such as lattice type, lattice rod thickness, and 2D shell thickness. Each factor would have at least three levels. The team already explored different lattice types and shell thicknesses, but not in the context of DOE. To evaluate each of the experiments, a response would need to be defined by the team.

Our team would also want to print a full-size metal version of our final design in Ti-64, but our budget did not allow us to do so. The cost of 3D metal printing our design in full scale would cost approximately $45,400.00, far more than the $1,000 limit we were given. If our team was able to print a metal version and a plastic version of our design and test each design's structural integrity, it would have been a better indicator of whether our design would fit inside the specifications of the telescope and would have been a more accurate representation of how our design will work when tested.

Moreover, with more time our team would conduct thermal testing to confirm material properties such as CTE. Finally, if given all the time we need, we would want to mount the structure onto a satellite and launch it deep into space, if L3Harris validates our model and deems it a valid optimized solution.

ACKNOWLEDGMENTS

The team would like to thank Professor Muir of the Mechanical Engineering Department at the University of Rochester, for helping our team troubleshoot problems with the NX software because of the complexity of our design, and for helping our team use the FaroArm for measurements.

We also want to thank Jim Alkins for his advice about 3D printing and for 3D printing test blocks for our team.

We would also like to thank Omar Soufan for providing our team with screws, inserts, and washers.

We want to thank Chris Pratt for helping with the bending test and for helping us order our 60% 3D printed model.

And finally, we would like to thank our sponsor Patrick Ellsworth for his help throughout our weekly meetings and for the opportunity to work with L3Harris.

REFERENCES

[1] Duncan, A. L., Kendrick, R. L., & Sigler, R. D. (n.d.). *US5905591A - Multi-Aperture Imaging System*. Google Patents. USPTO report Retrieved April 10, 2022, from https://patents.google.com/patent/US5905591A

[2] Basu, S. (n.d.). *US20050088734A1 - Autonomously Assembled Space Telescope*. Google Patents. USPTO report Retrieved April 10, 2022, from https://patents.google.com/patent/US20050088734A1

[3] Rojek, Izabela et al. "Optimization of Extrusion-Based 3D Printing Process Using Neural Networks for Sustainable Development." *Materials (Basel, Switzerland)* vol. 14,11 2737. 22 May. 2021, doi:10.3390/ma14112737

[4] Carlota, V. "What Is the Environmental Impact of Metal Additive Manufacturing?" *3Dnatives*, 4 Dec. 2020, https://www.3dnatives.com/en/environmental-impact-metal-additive-manufacturing-

APPENDIX A

Work Breakdown Structure

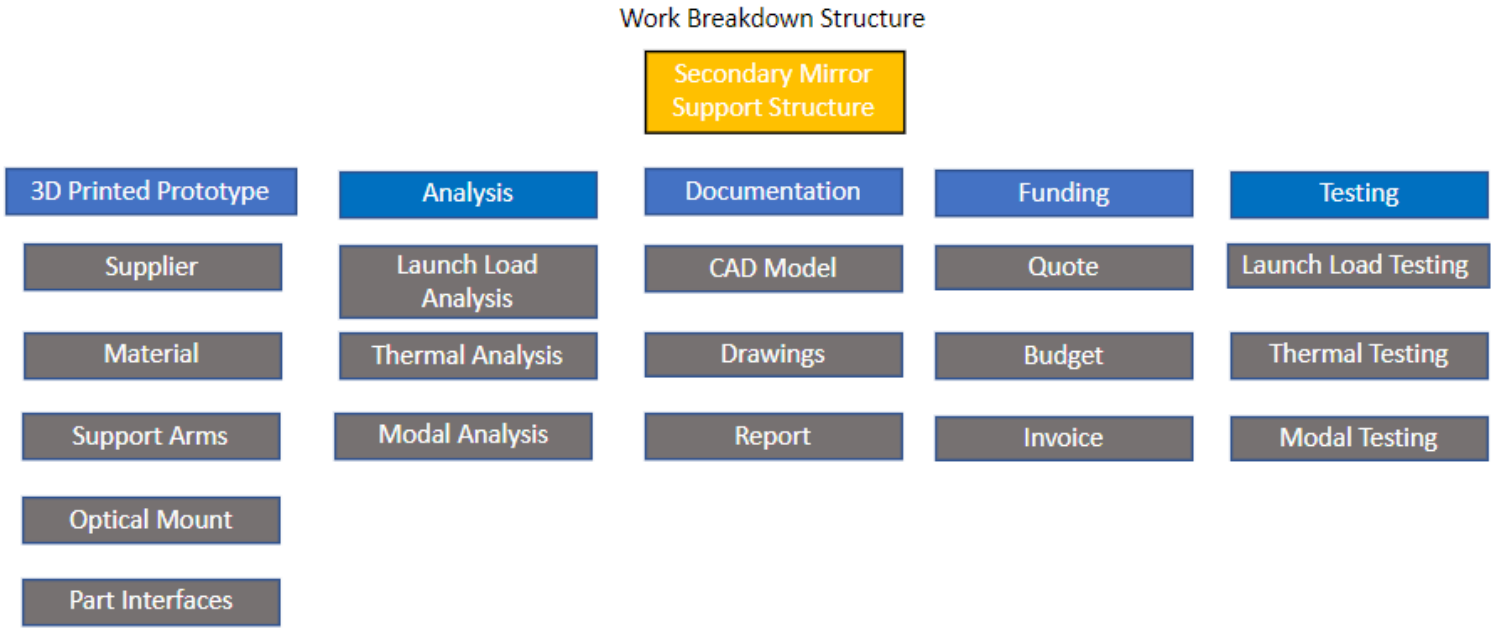

APPENDIX B

Critical Path Management

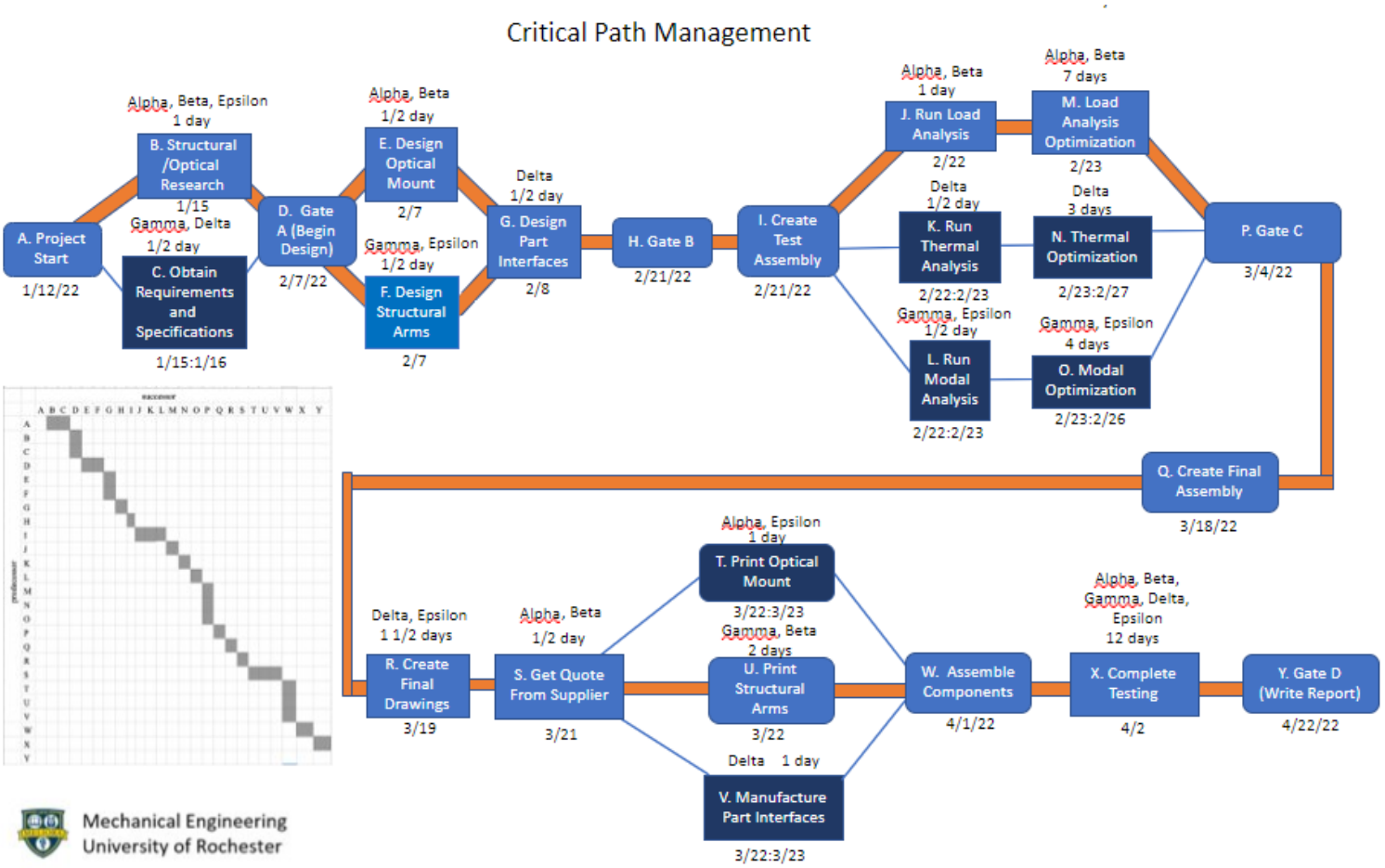

APPENDIX C

Concept Design I – I-Beam Cross Section Structure

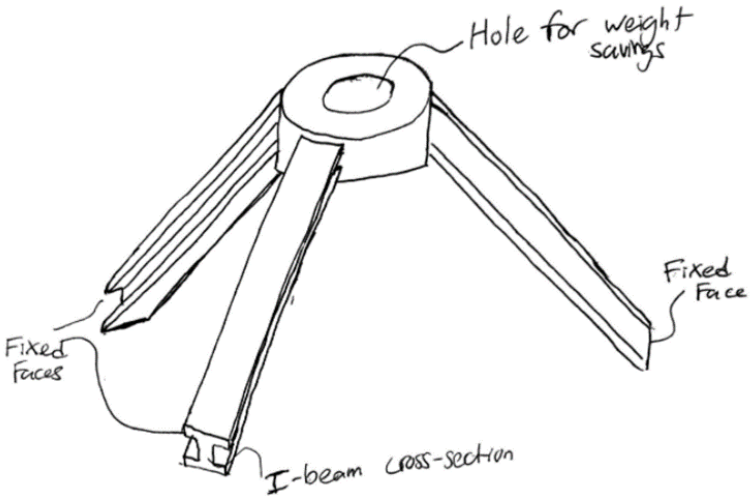

Problem:
Design SMSS

Conclusion:
Part does not fail under specified loads.

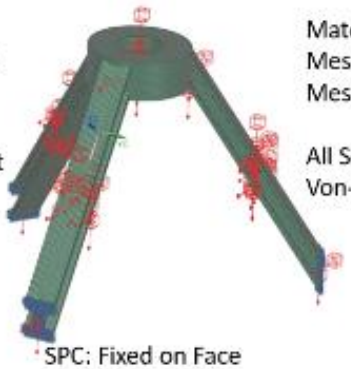

Material: Titanium Alloy
Mesh: 10-node Tetr.
Mesh Size: 0.4 in

All Sols. Elemental-Nodal Von-Mises Stress

SPC: Fixed on Face

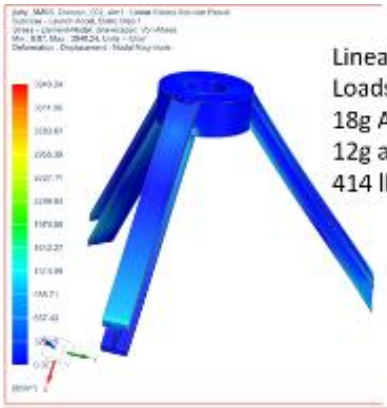

Linear Statics Sol.
Loads:
18g Applied axially
12g applied laterally
414 lbf applied for SM

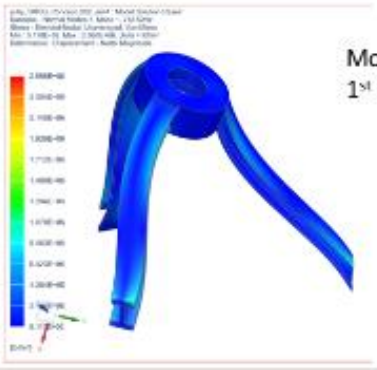

Modal Analysis Sol.
1st Mode: 212 Hz

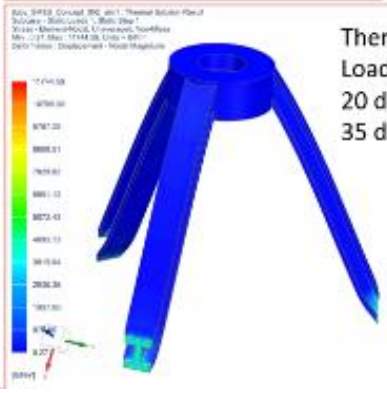

Thermal Stress Sol.
Loads:
20 deg C resting
35 deg C load

APPENDIX D

Concept Design II –Solid Center Structure

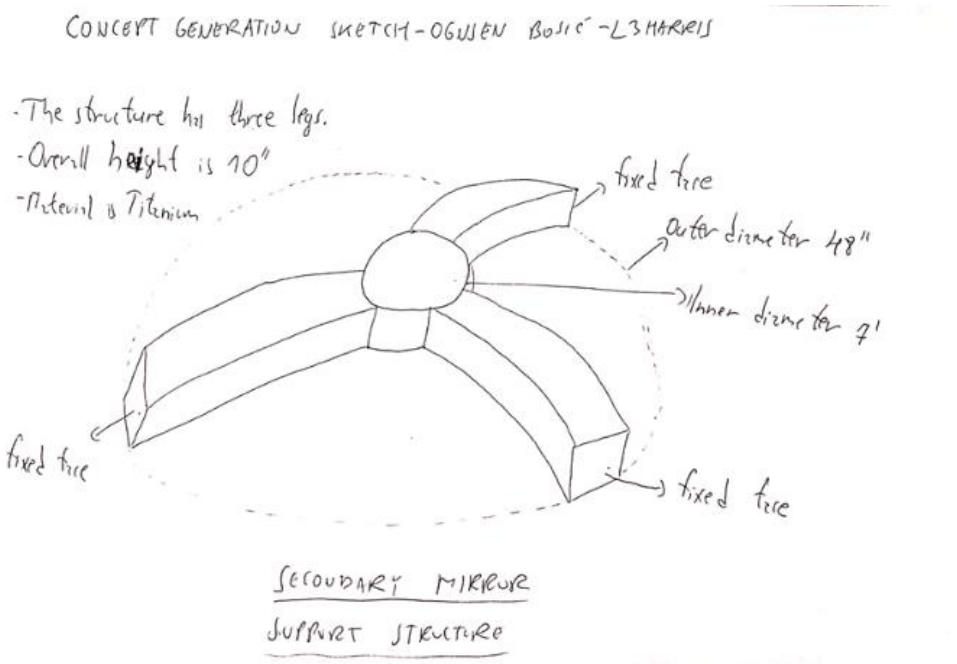

Problem Statement: SMSS needs to be design
Conclusions: This concept satisfies all the stress specifications.

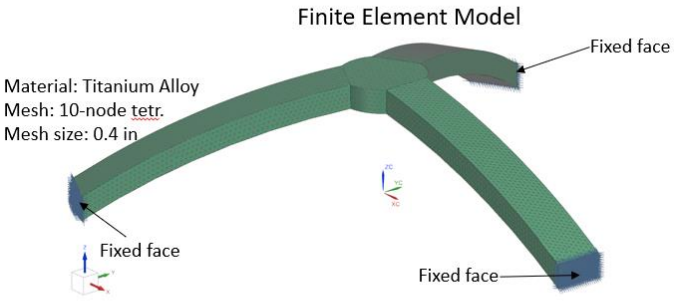

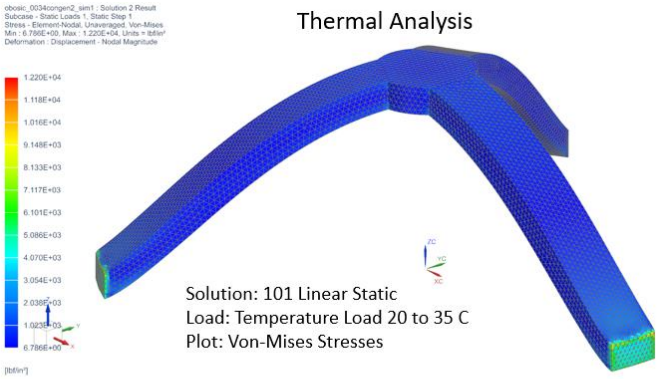

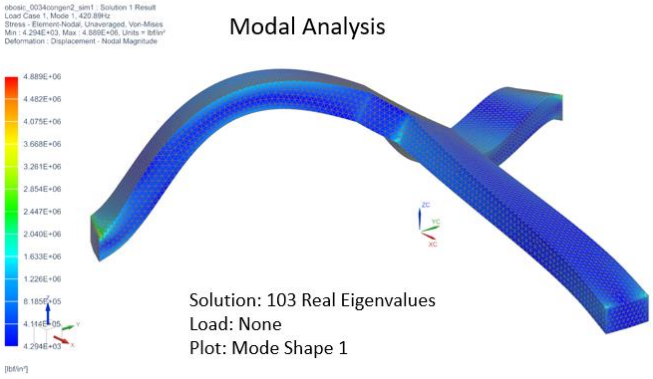

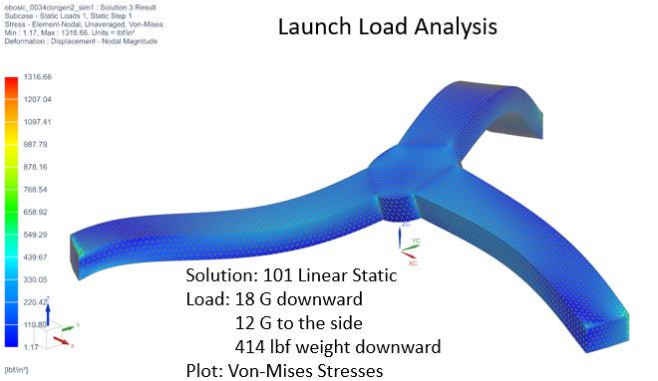

APPENDIX E

Concept Design III –Double Cylinder Structure

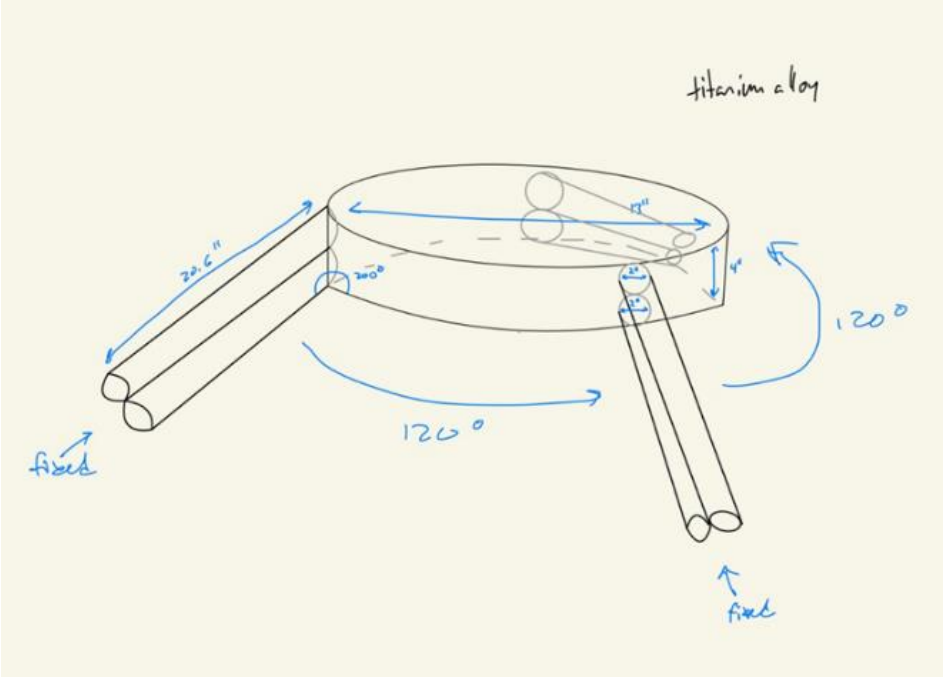

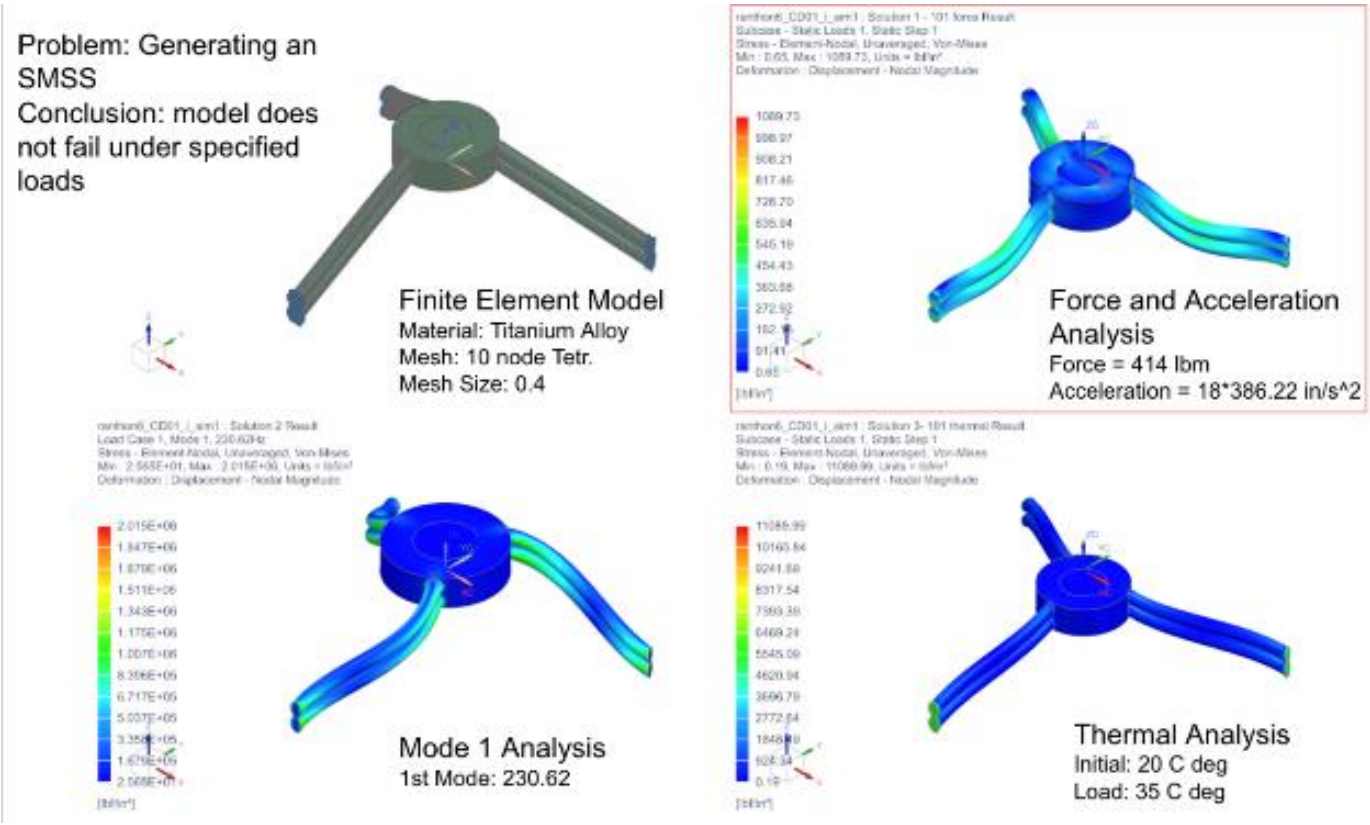

APPENDIX F

Concept Design IV –Tapered Support Leg Structure

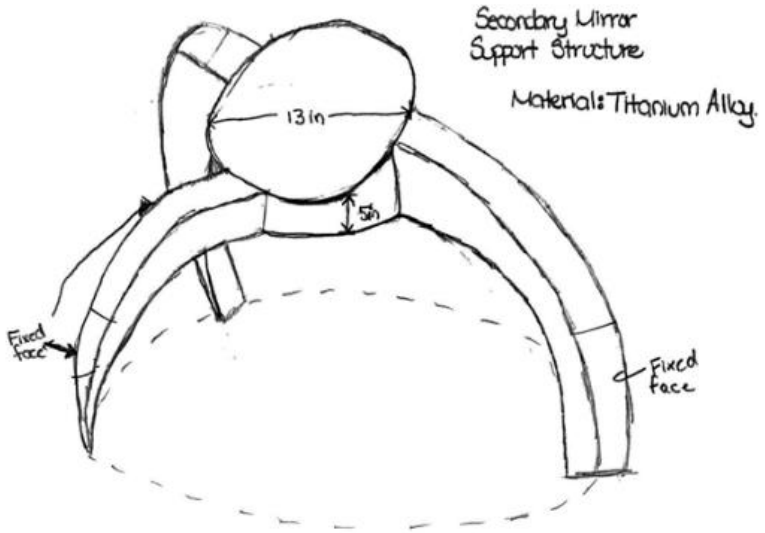

Problem: Design a Secondary Mirror Support Structure.

Conclusion: Part does not fail under specified thermal load

Finite Element Model

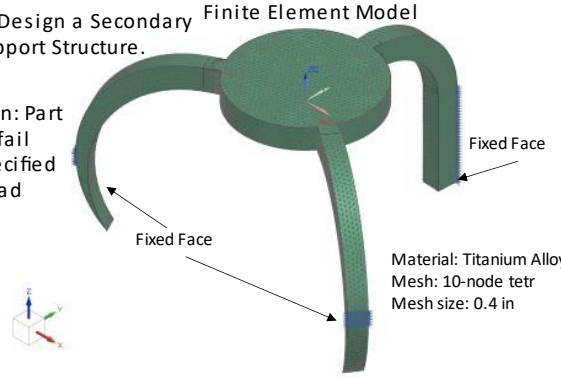

Material: Titanium Alloy
Mesh: 10-node tetr
Mesh size: 0.4 in

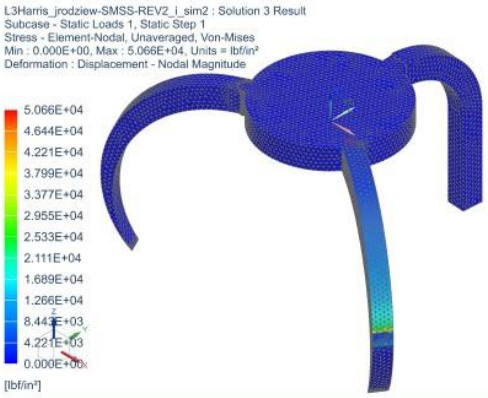

Force Analysis

Force= 414 lbm
Acceleration= 18*386.22 in/s^2
18G downward

Modal Analysis
Load: None
1st Mode: 19.66 Hz

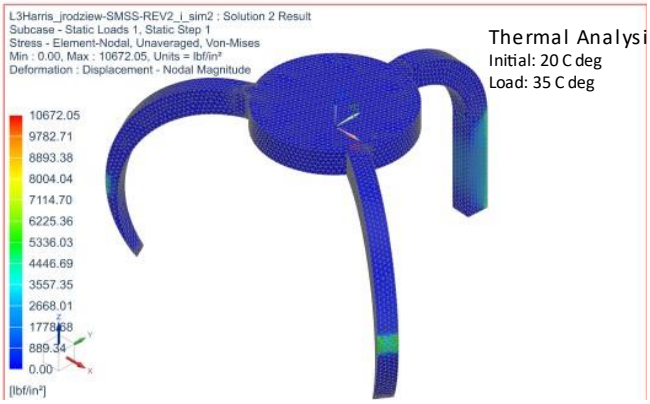

Thermal Analysis
Initial: 20 C deg
Load: 35 C deg

APPENDIX G

Concept Design V –Doughnut Structure

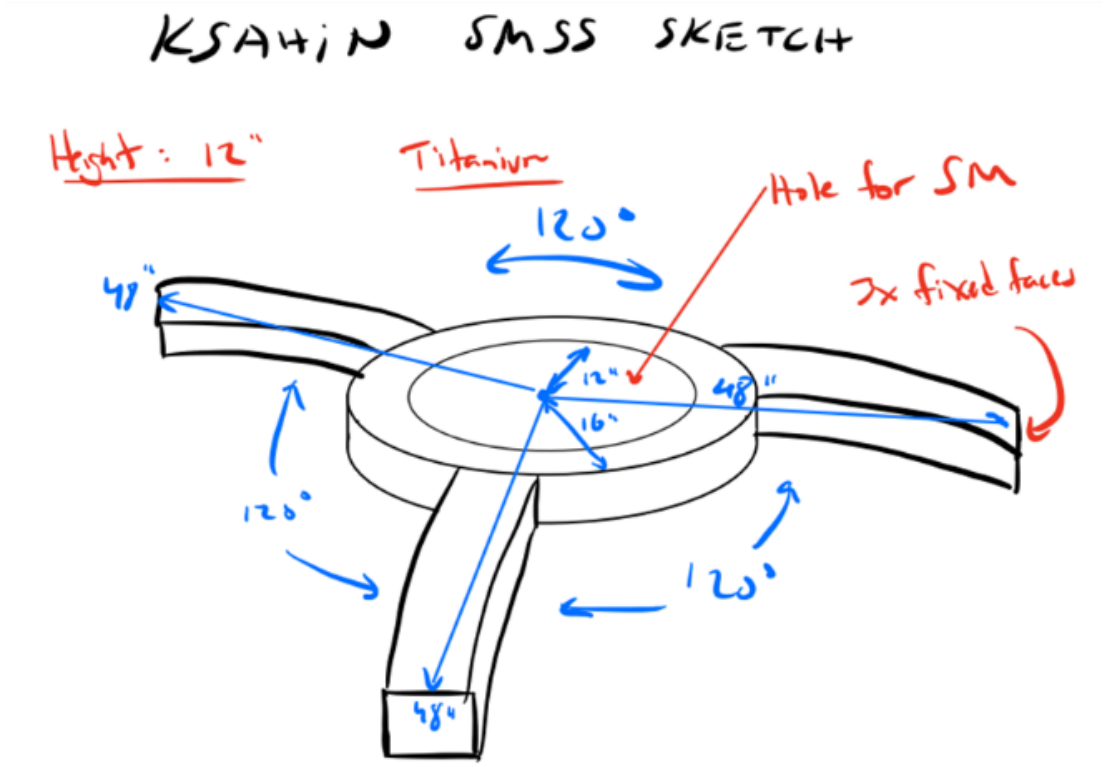

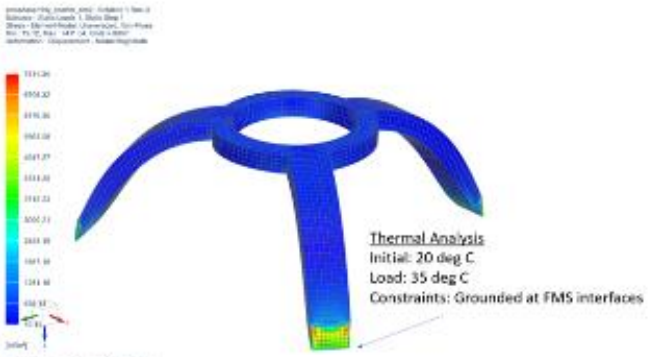

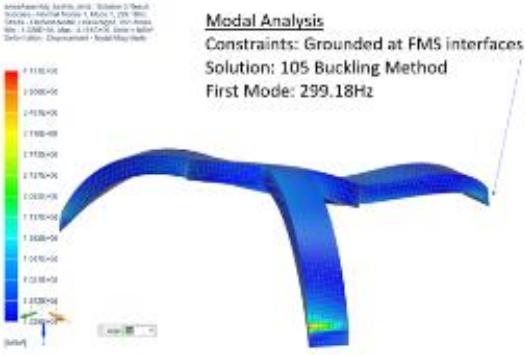

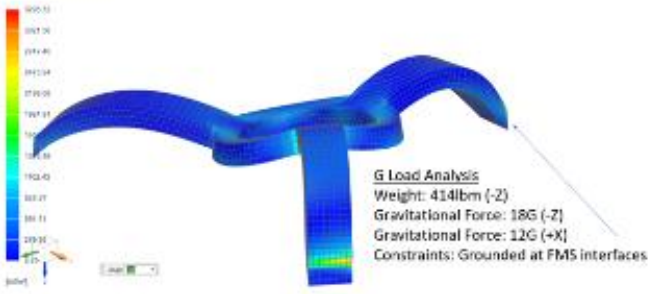

APPENDIX H

Illustration of Lockheed Martin WorldView-4 Satellite, with Emphasis on the Secondary Mirror Support Structure

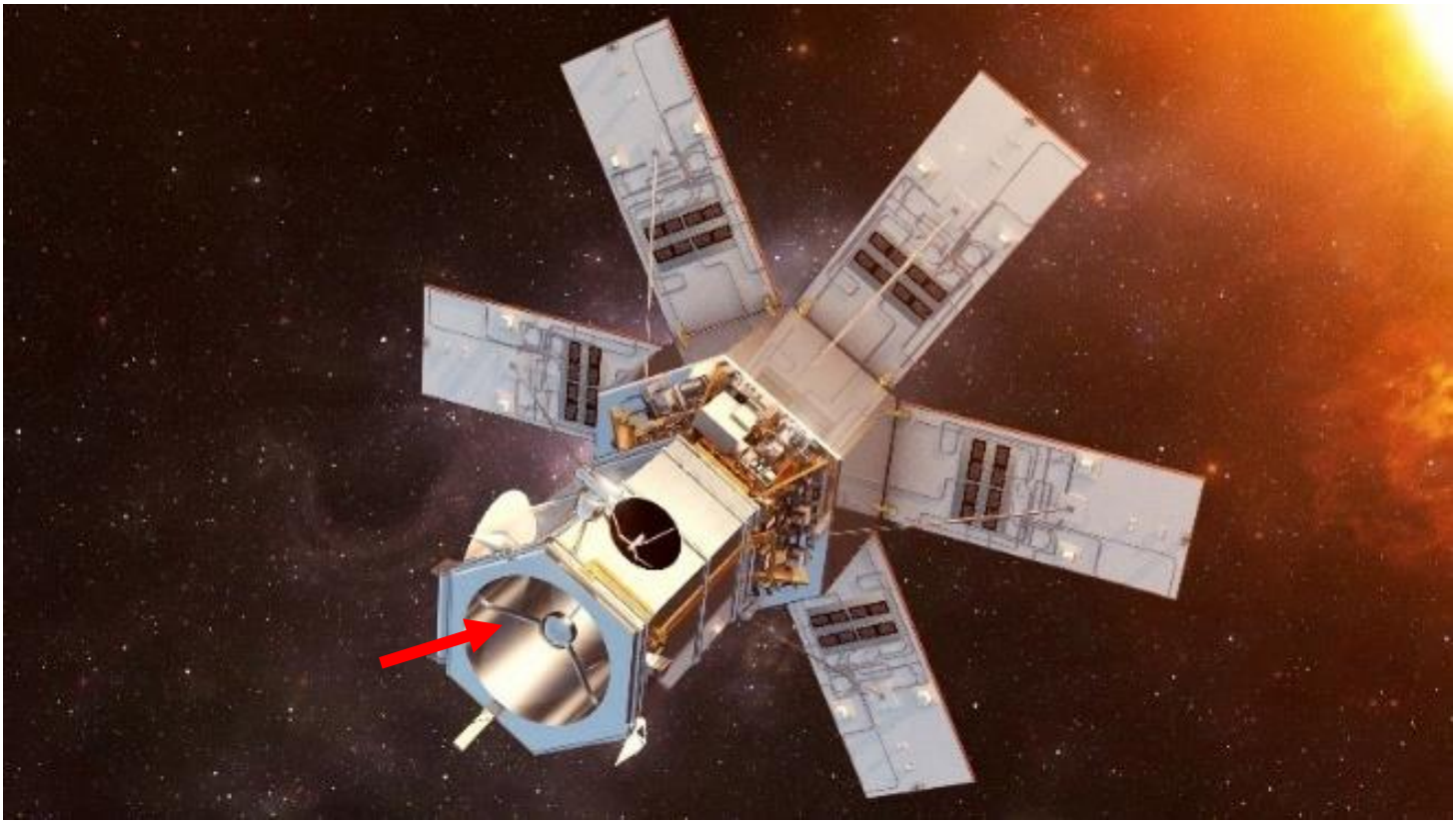

APPENDIX I

Preliminary Machine Drawing of Concept V Used for Initial ROM

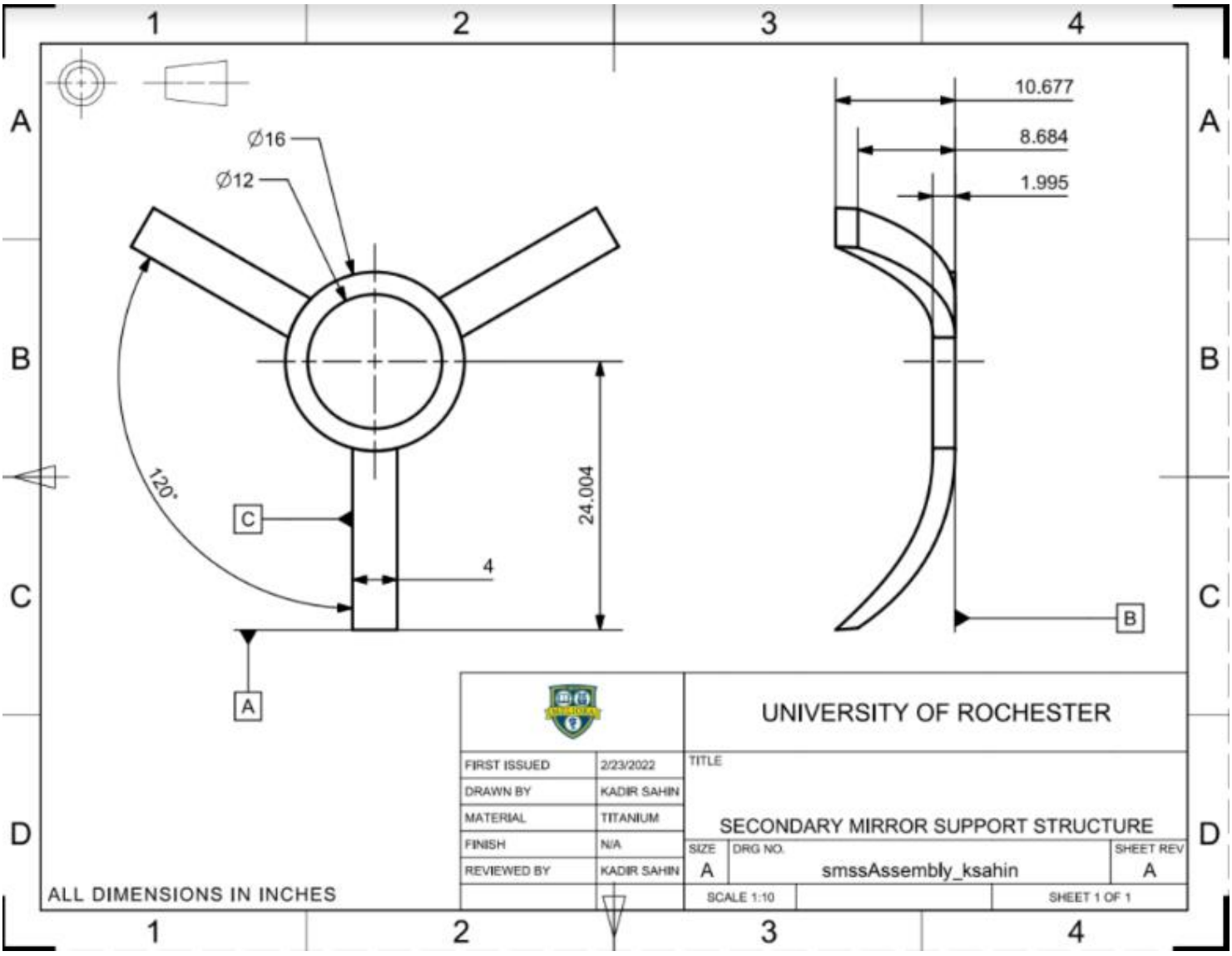

APPENDIX J

Full-Scale Solid Body SMSS Print in Titanium Quote

The ROM quote is **$45,400.** This is to print the part with Ti 6Al 4V rather than Invar.

What this includes:

1. Engineering Services & Project Management
2. Material
3. EBAM Production
4. Dimensional Scan
5. Stress Relief / Heat Treat
6. Crating and shipping

Not Included:

1. Machining	Additional $8,000 – $10,000
2. NDT – X-Ray, etc.	Additional $1,000 – $2,000
3. Dimensional Inspection	Additional $3,500

APPENDIX K

Pre-Topology Optimized Model vs. Post-Topology Optimized Model

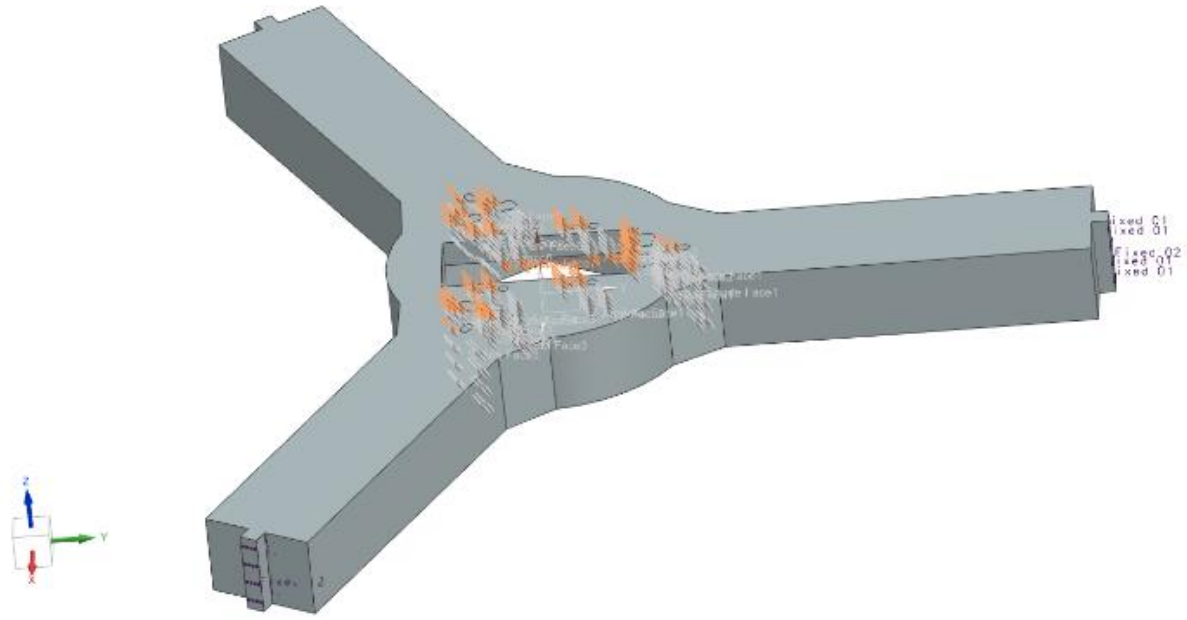

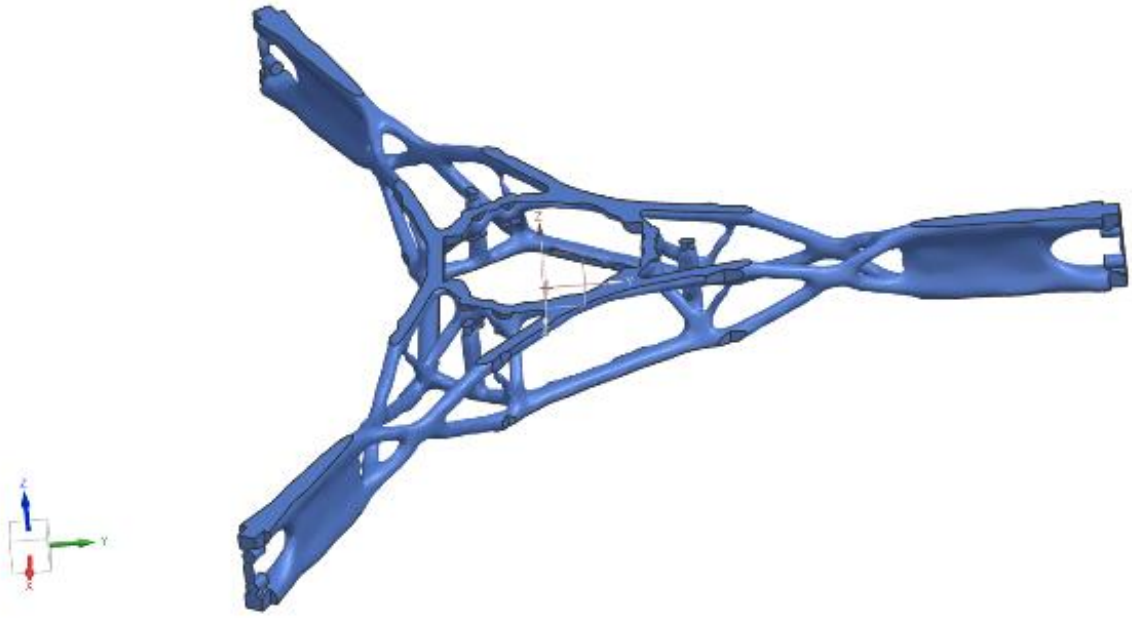

APPENDIX L

NX Illustration of Three Different Lattices with Stiffness and Porosity

TriDiametral Lattice:

Porosity: 96%
Stiffness in X : 7
Stiffness in Y : 4
Stiffness in Z : 4

BiTriangle:

Porosity: 95%
Stiffness in X : 22
Stiffness in Y : 20
Stiffness in Z : 53

QuadDiametral:

Porosity: 95%
Stiffness in X : 14
Stiffness in Y : 14
Stiffness in Z : 14

APPENDIX M

Final Model: Finite Element Analysis Configuration

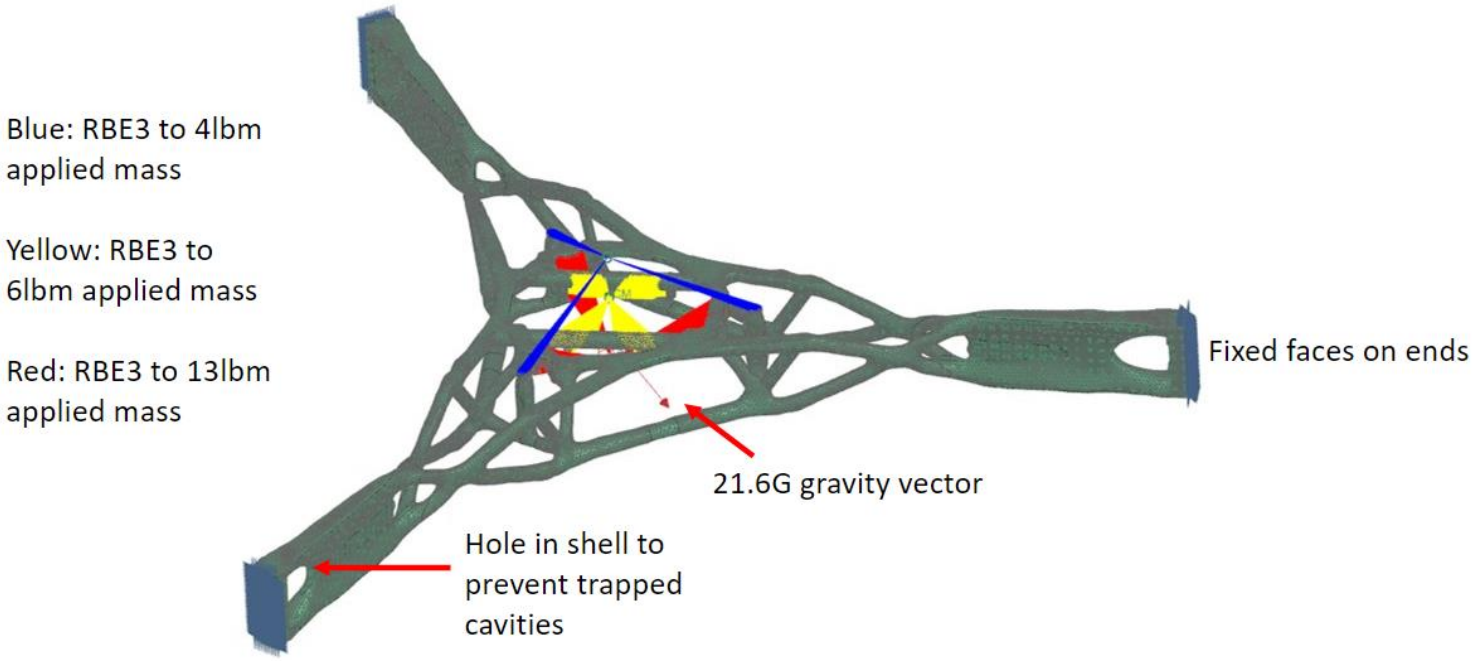

APPENDIX N

Final Model: Modal Solution (124 Hz)

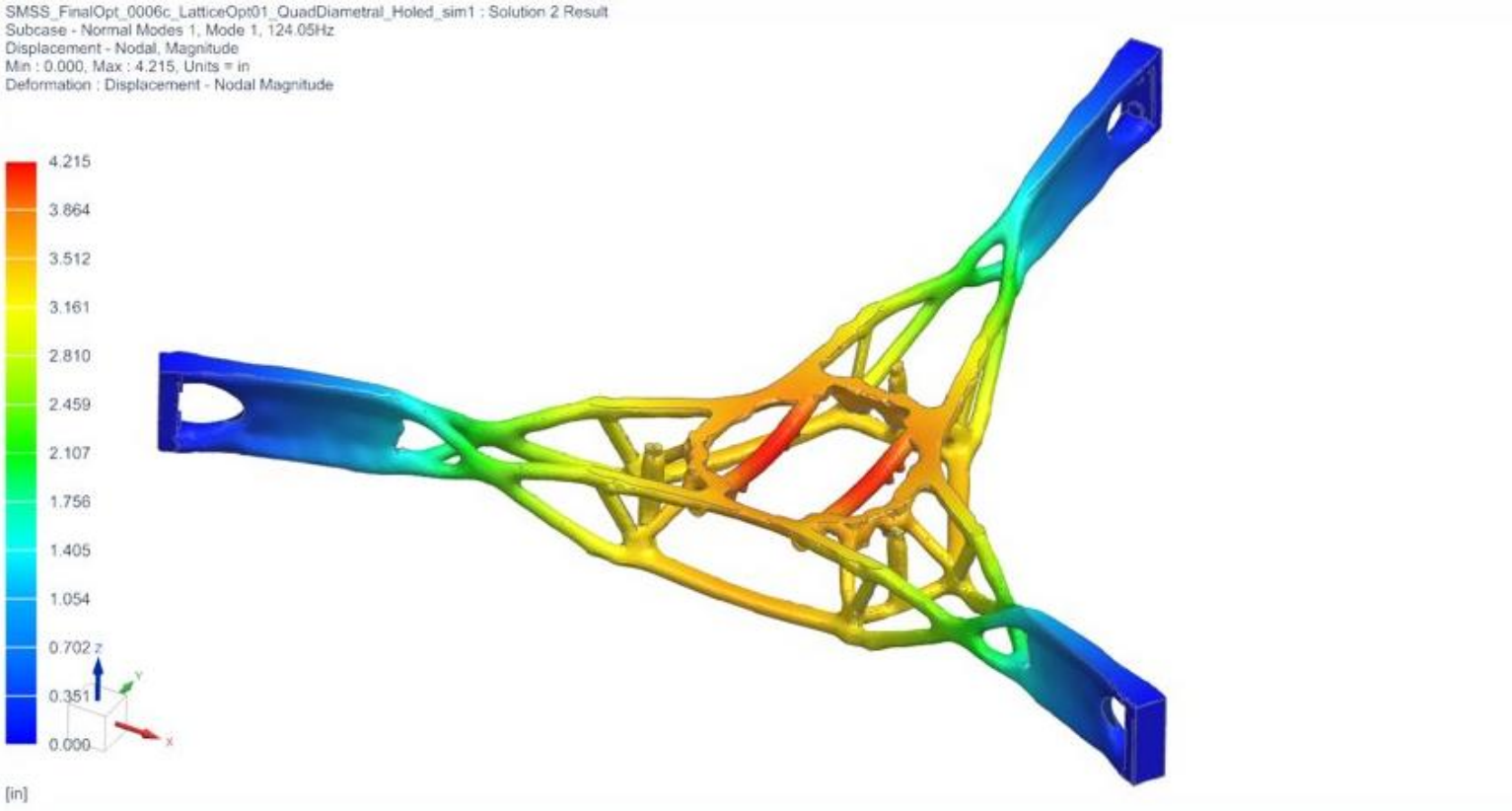

APPENDIX O

Final Model: Von-Mises Stress Solution (23,170 psi)

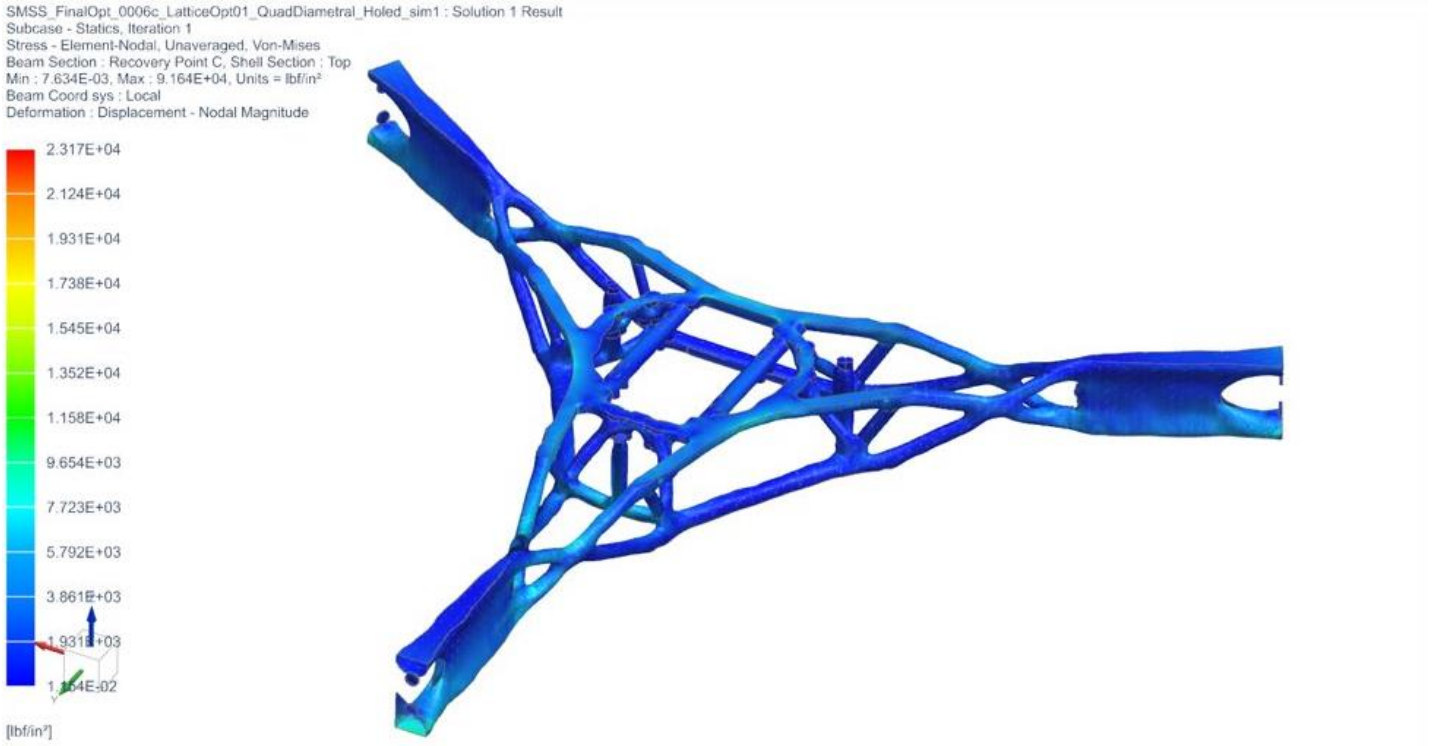

APPENDIX P

Final Model: Buckling Solution

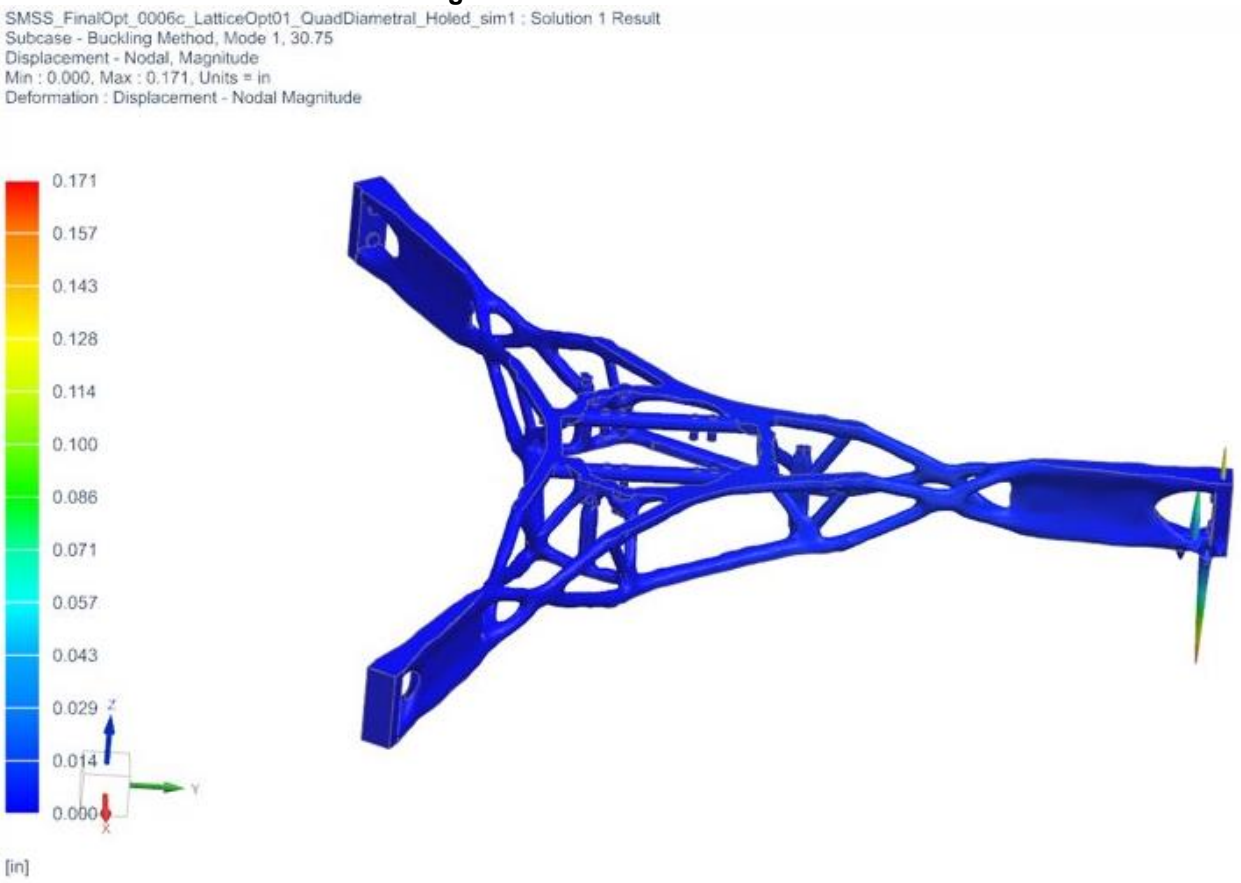

APPENDIX Q

Final Model: Max Stress Solution- Lattice Only

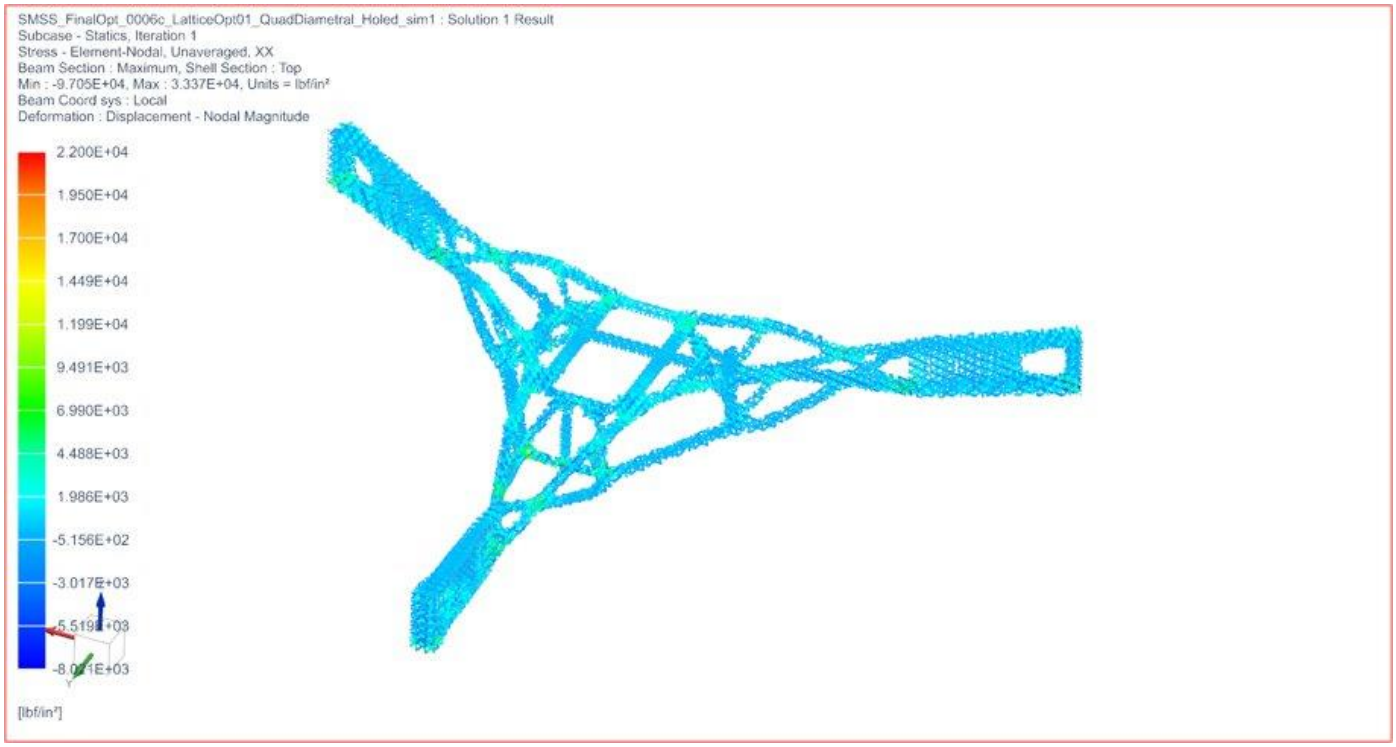

APPENDIX R

Tolerance Analysis Testing

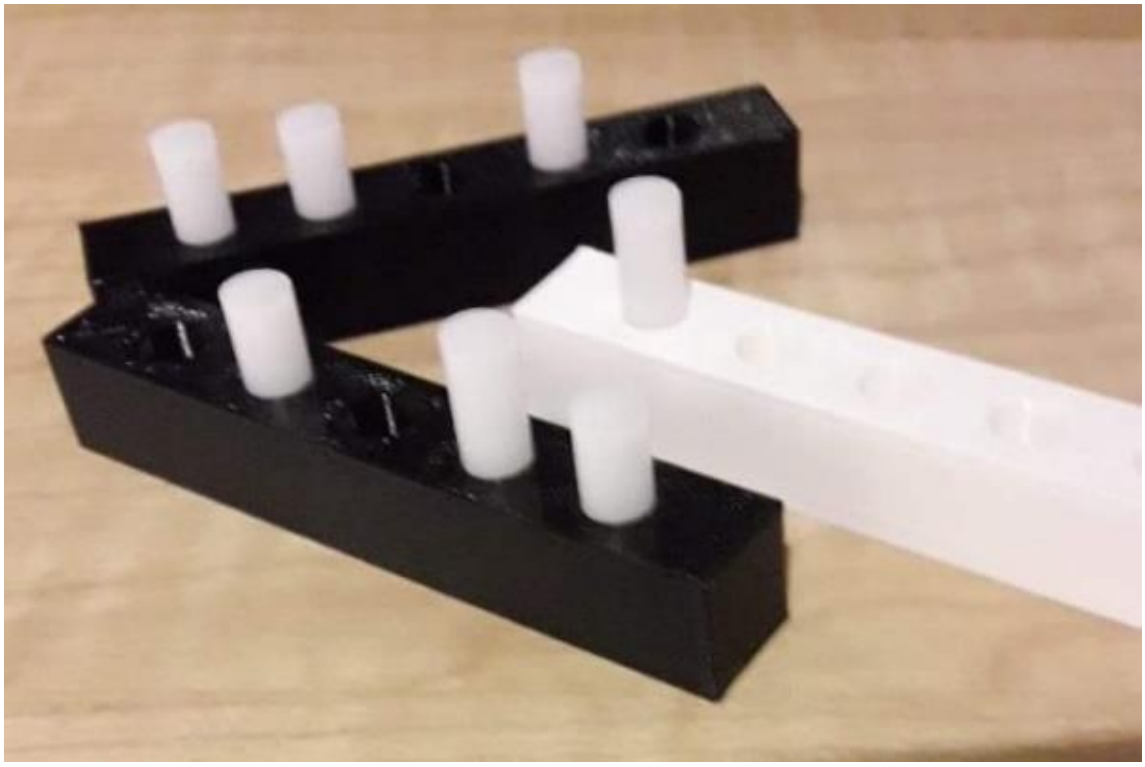

APPENDIX S
FaroArm

APPENDIX T

Printed 60% scale ABS-M30 prototype with labeled holes

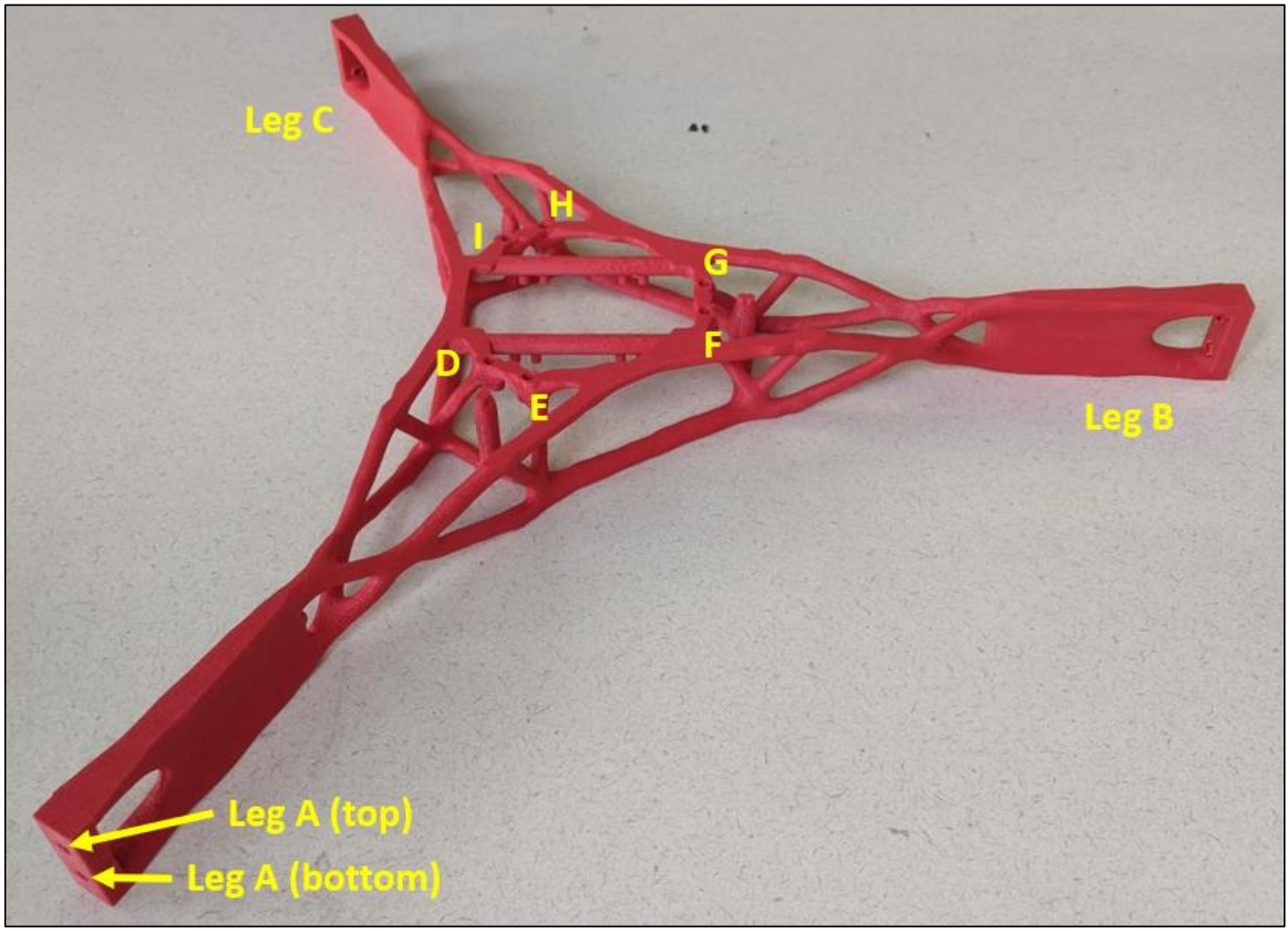

APPENDIX U

Milling Process of Mounting Legs and Finished Mounting Legs

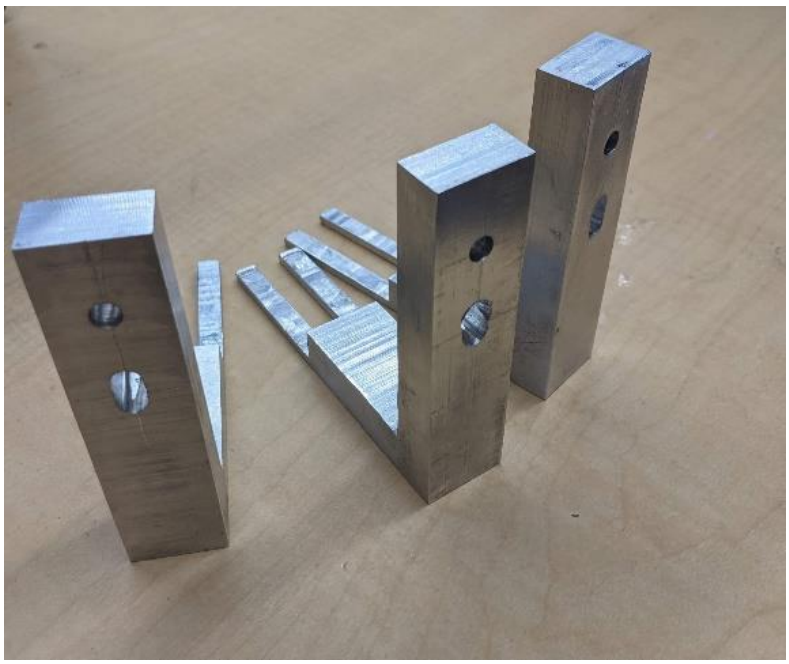

APPENDIX V

BiTriangle Lattice Bending Test

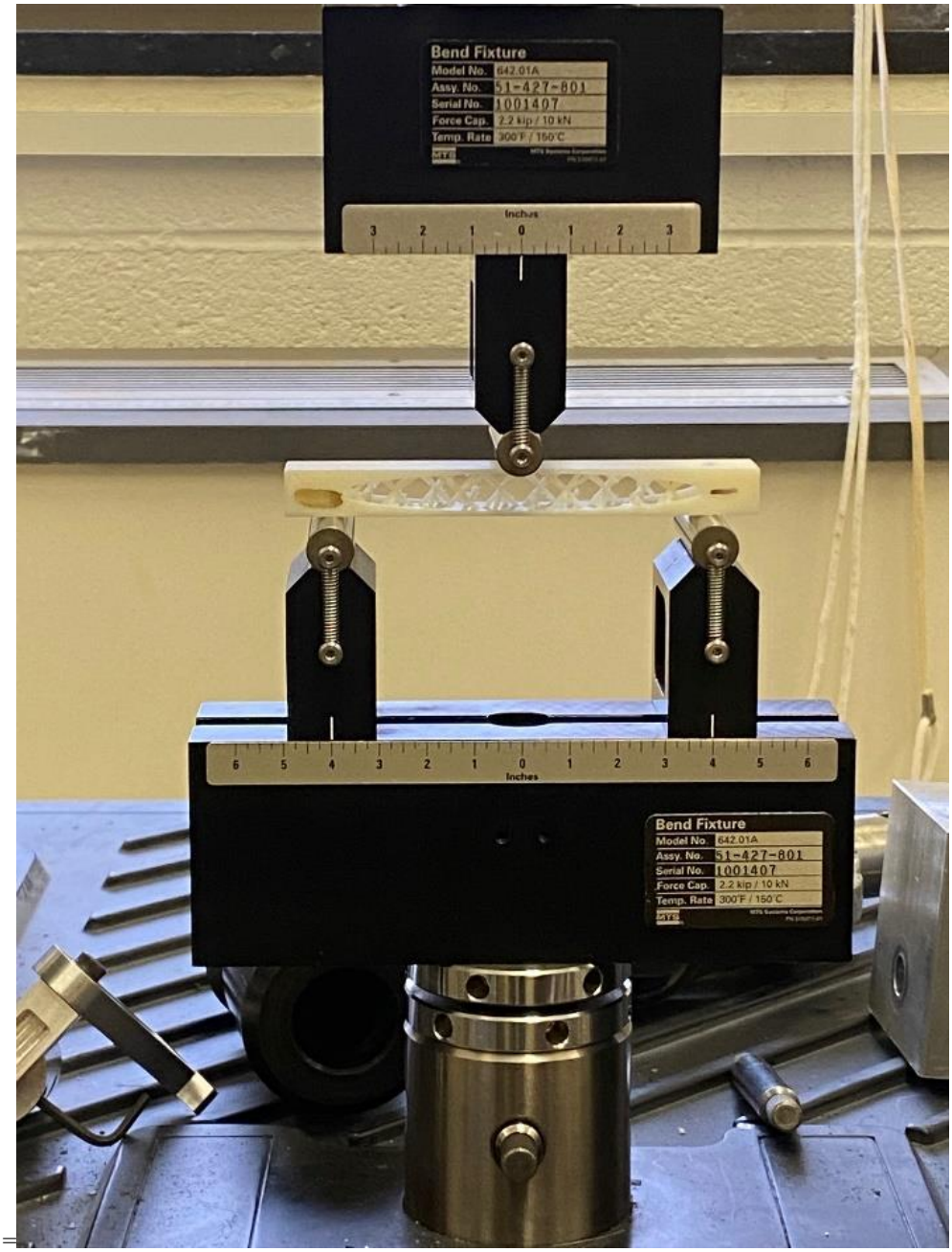

APPENDIX W

Force-Displacement Graph of Each Sample

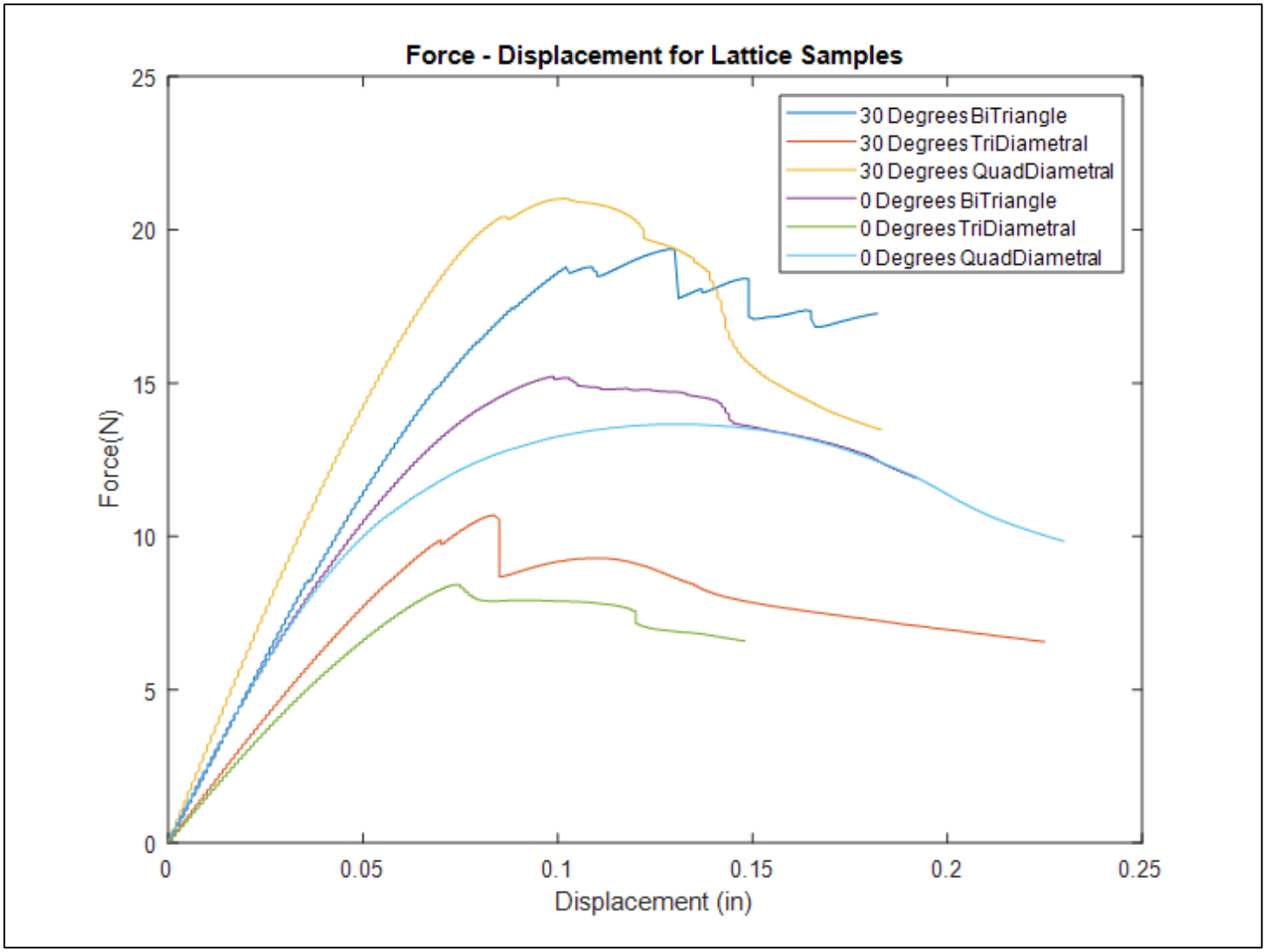

APPENDIX X

Printed Lattice Test Blocks and CAD Lattice Blocks

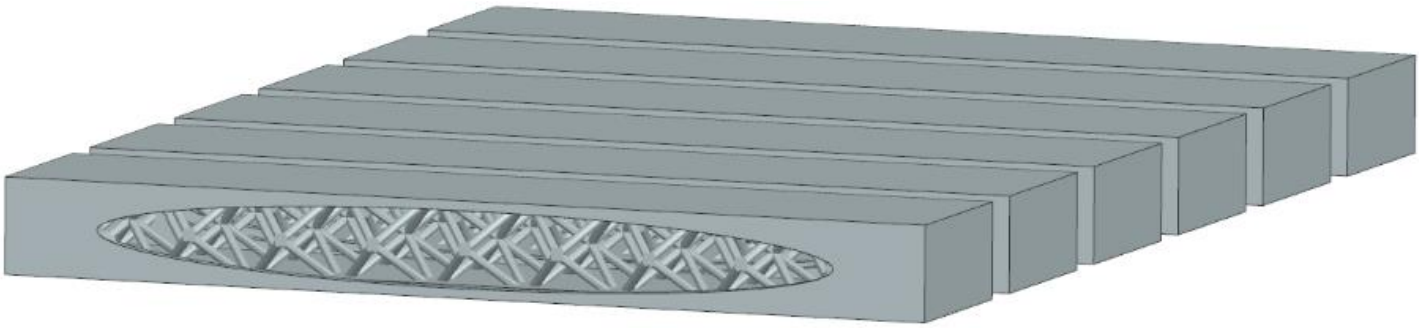

APPENDIX Y

Final 3D Printed Design Mounted on Newport Table

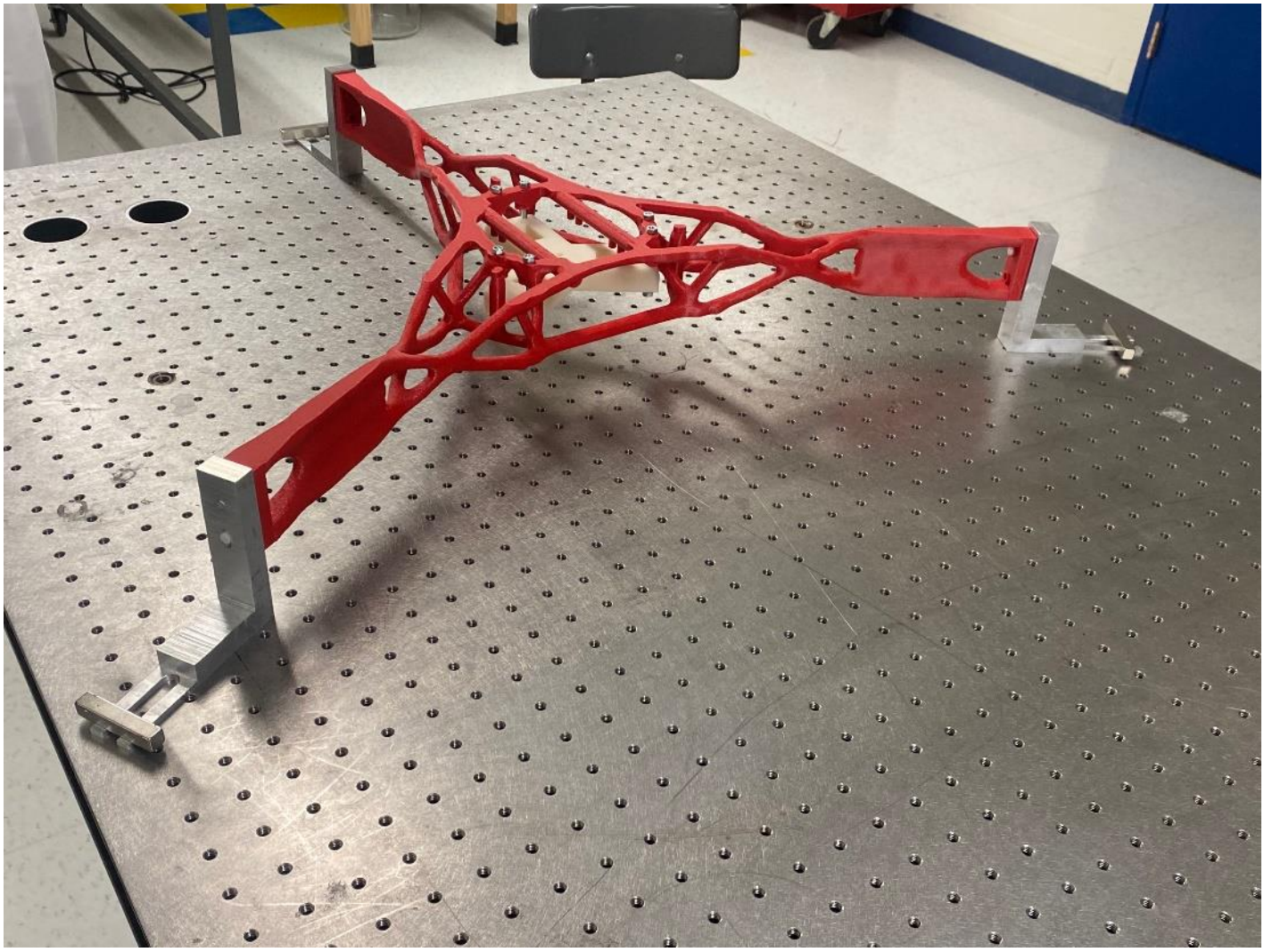

APPENDIX Z

Final Design Vertical and Horizontal Displacement Test

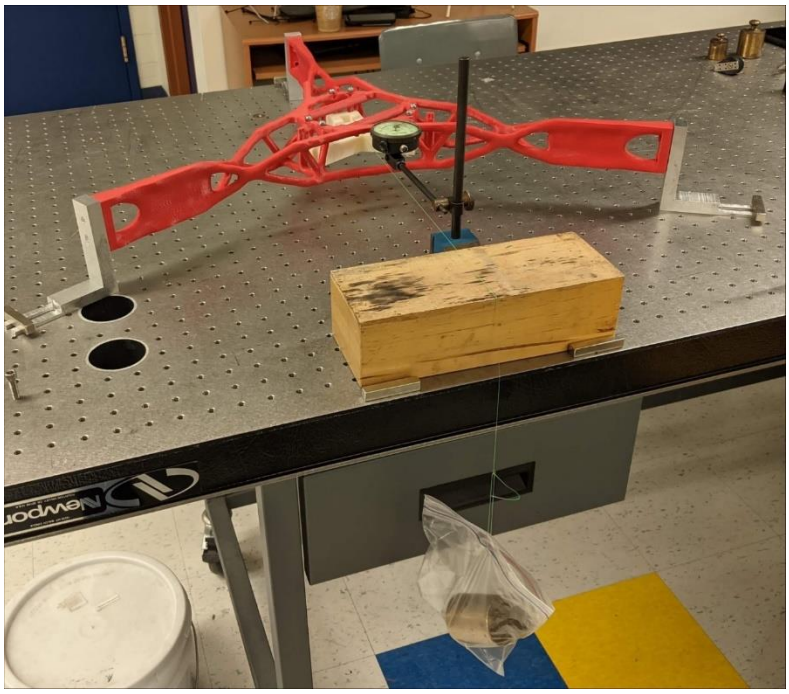

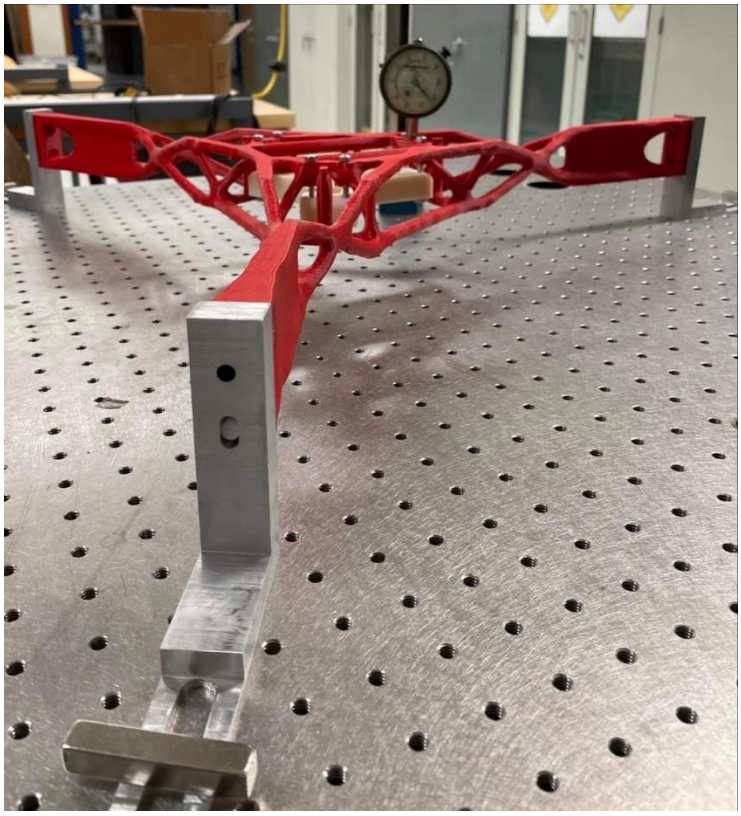

APPENDIX AA

Final Design Vertical Displacement Test: Force (lbf) vs. Displacement (inches)

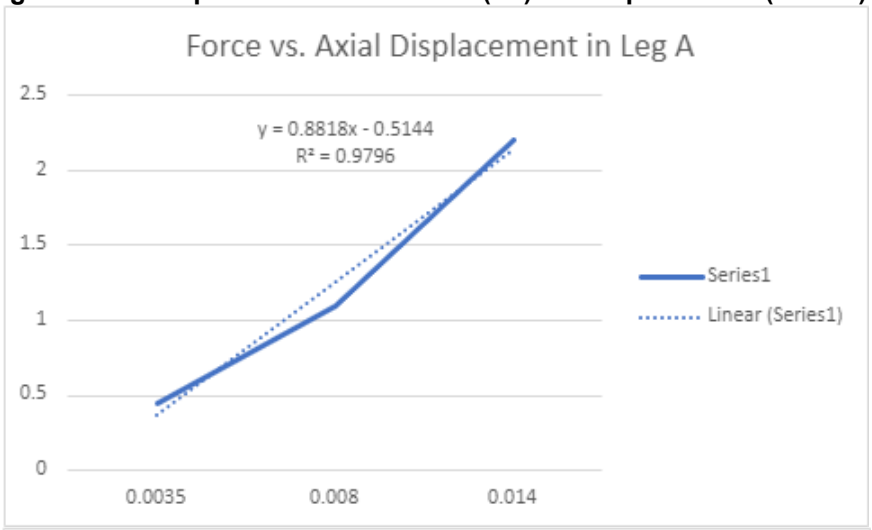

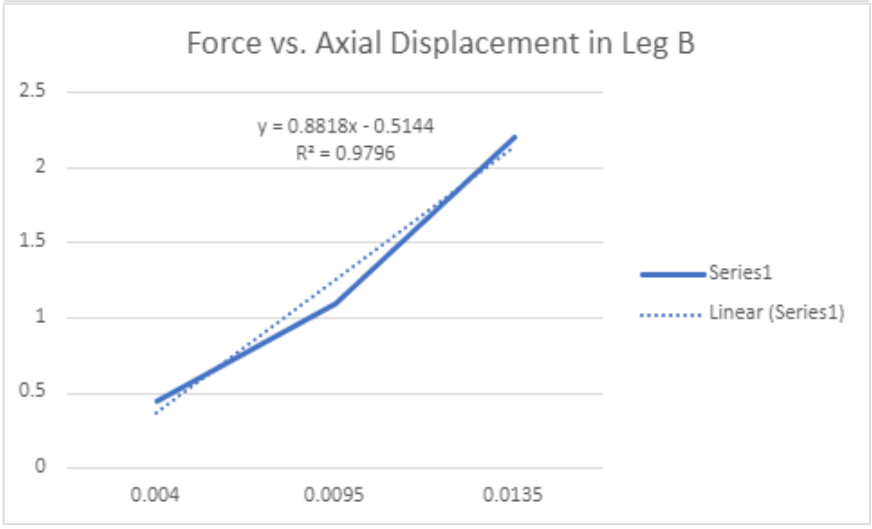

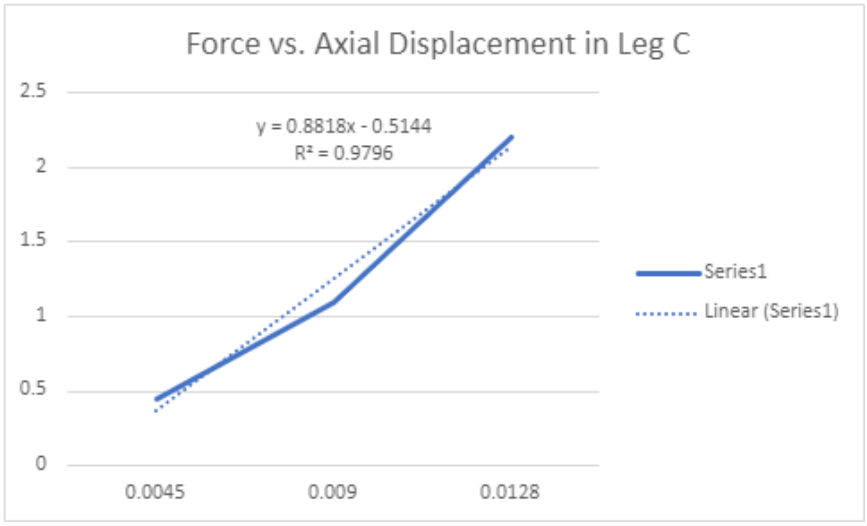

APPENDIX BB

Final Design Horizontal Displacement Test: Force (lbf) vs. Displacement (inches)

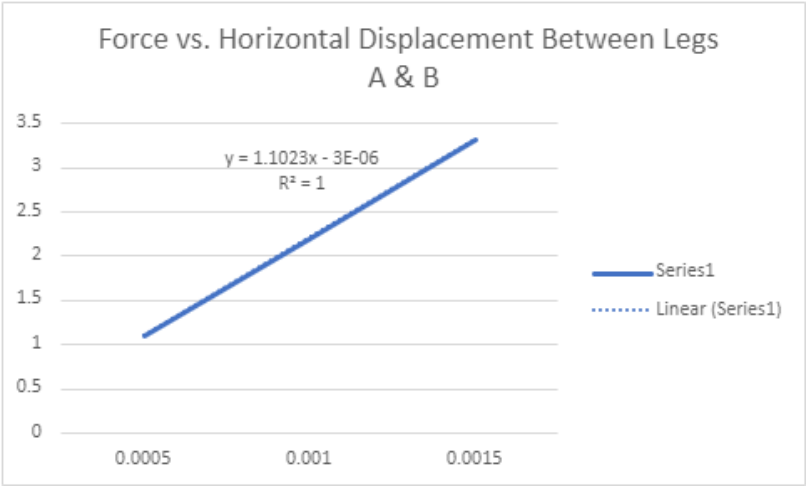

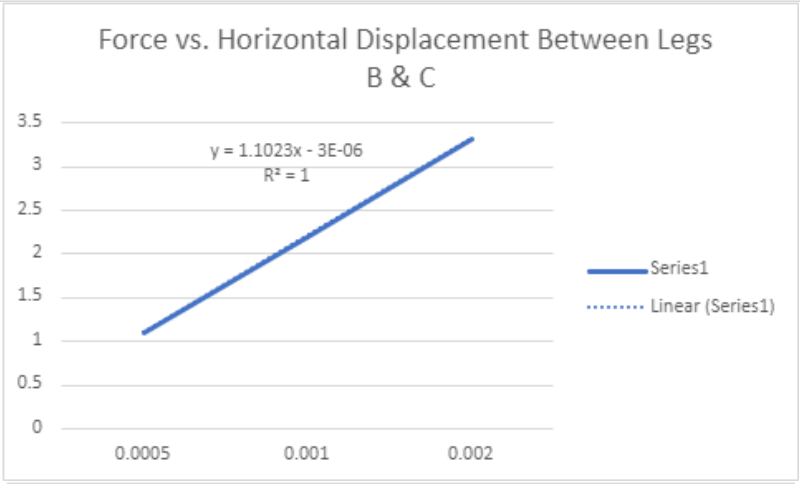

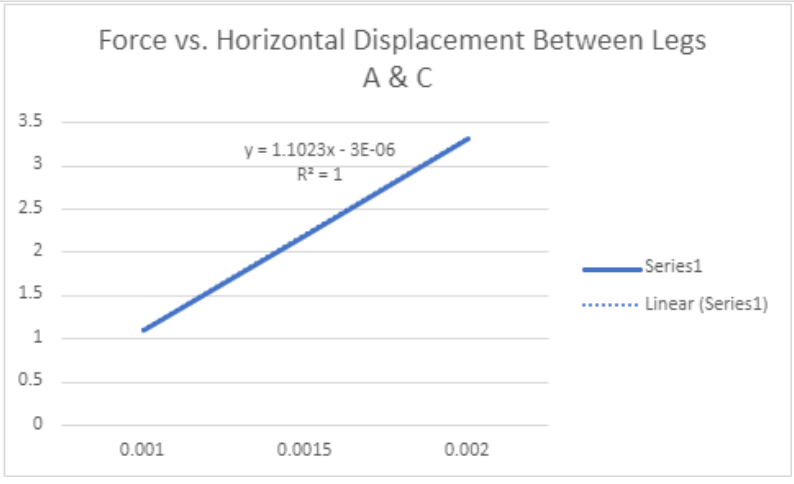

APPENDIX CC

Modal Simulation Set-up with Accelerometer

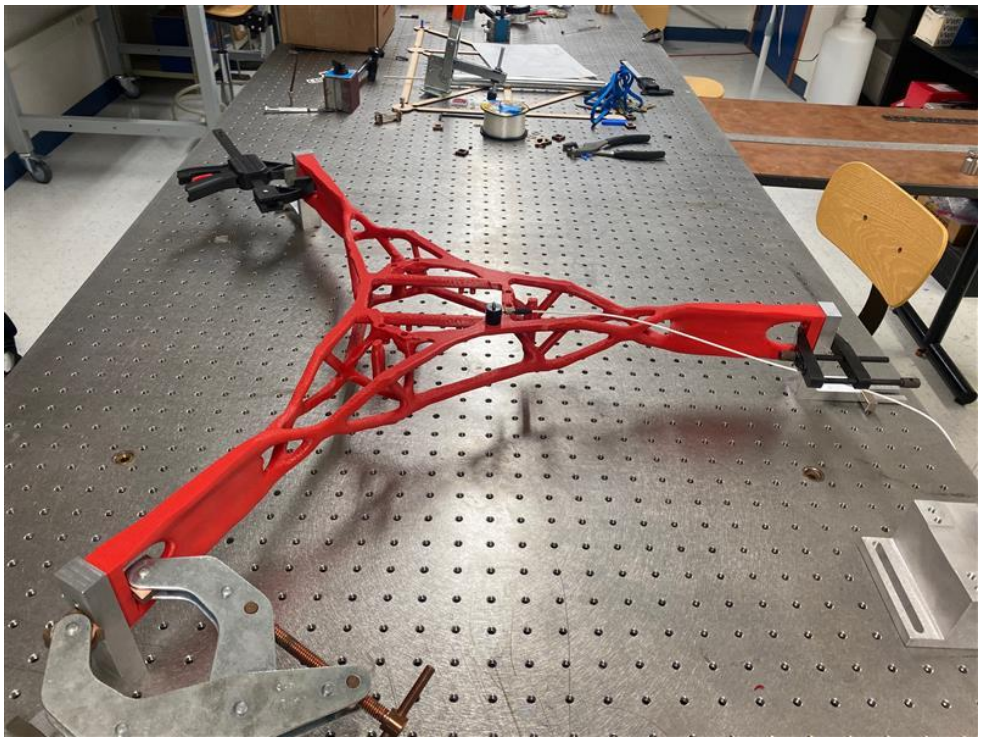

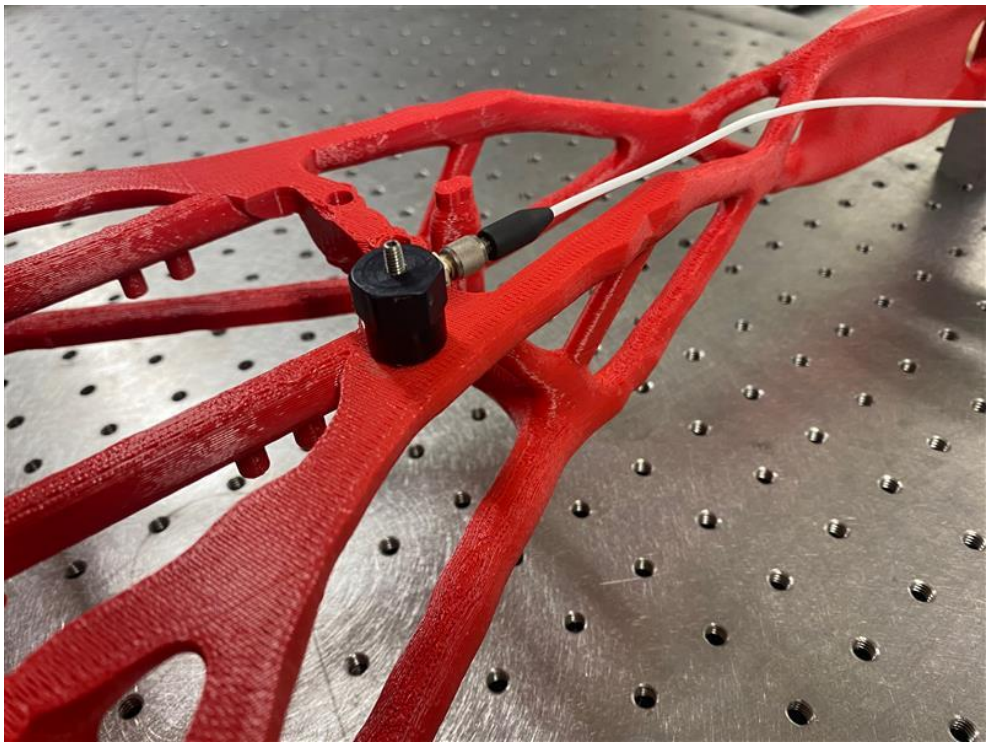

APPENDIX DD

Modal Test Results for 60% Scaled Print

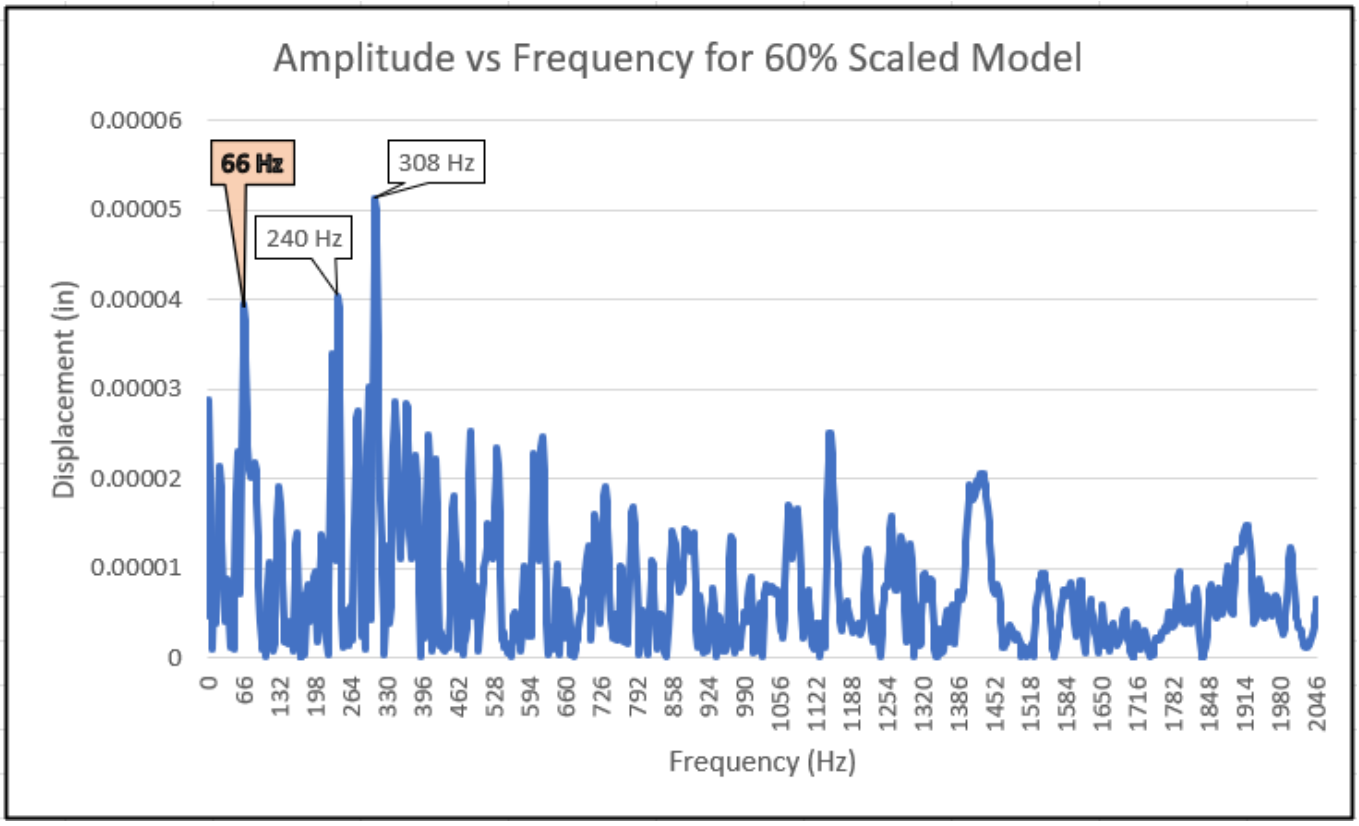

APPENDIX EE

60% Reduced SMSS Final Print in ABS-M30

APPENDIX FF

Drawing of 60% Reduced SMSS

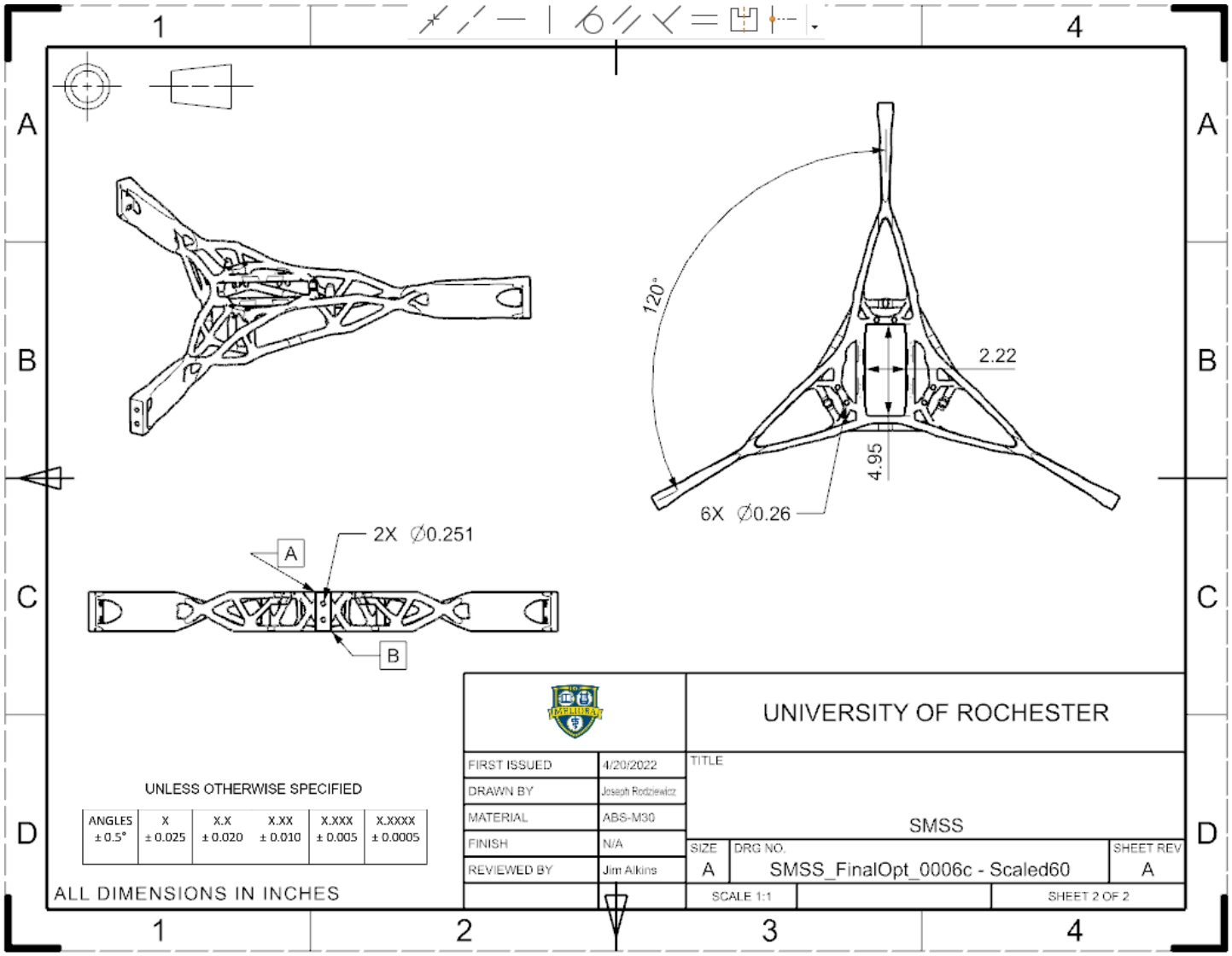

APPENDIX GG

Drawing of 20% Reduced SMSS

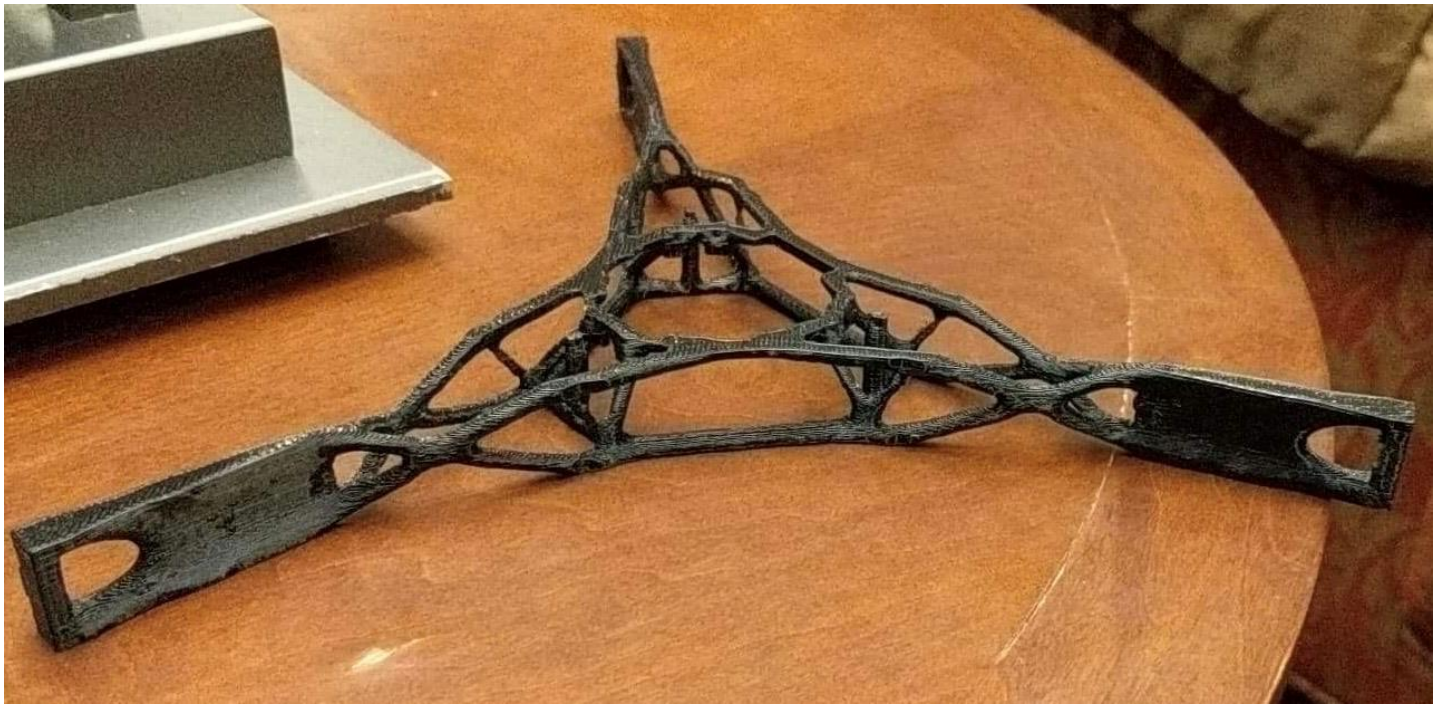

APPENDIX HH

Aluminum scrap sample from which the mounting legs were fabricated & Finished Mounting Legs

APPENDIX II

Manufacturing Drawing of Mounting Leg

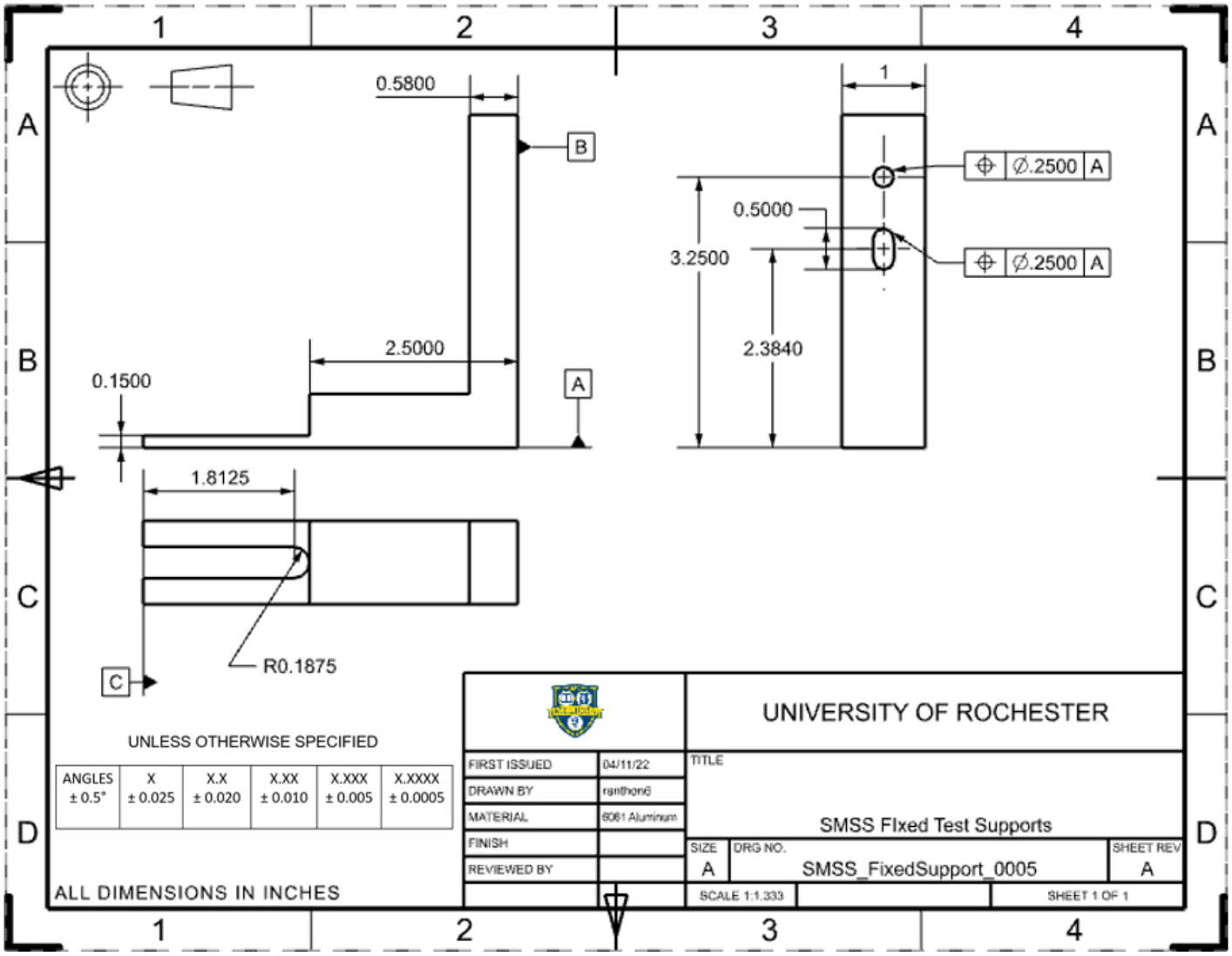

APPENDIX JJ

Printed Load Plate with Screws and Bolts Attached

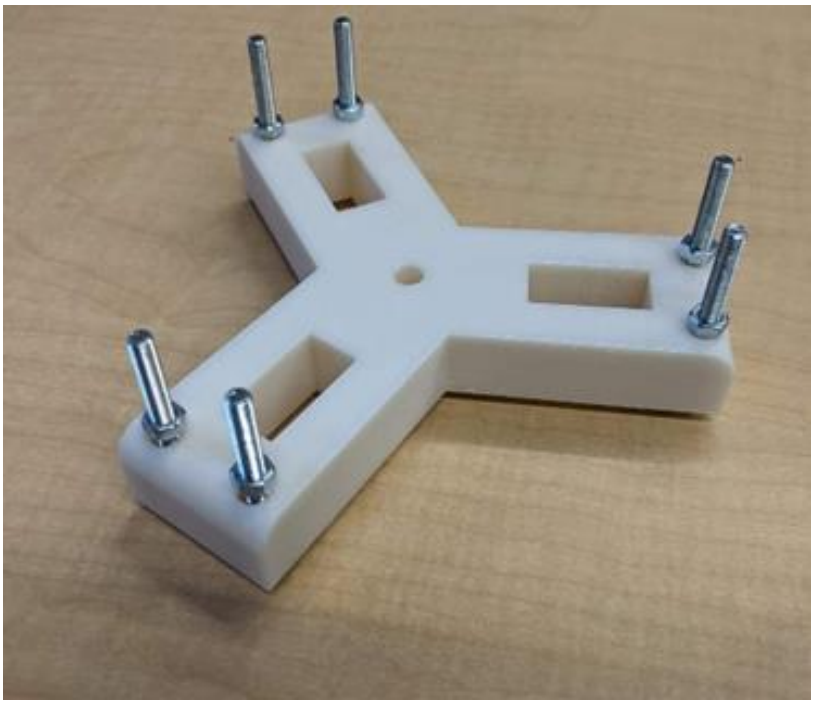

APPENDIX KK

Patent Design Pictures from Lockheed Martin Company[1]

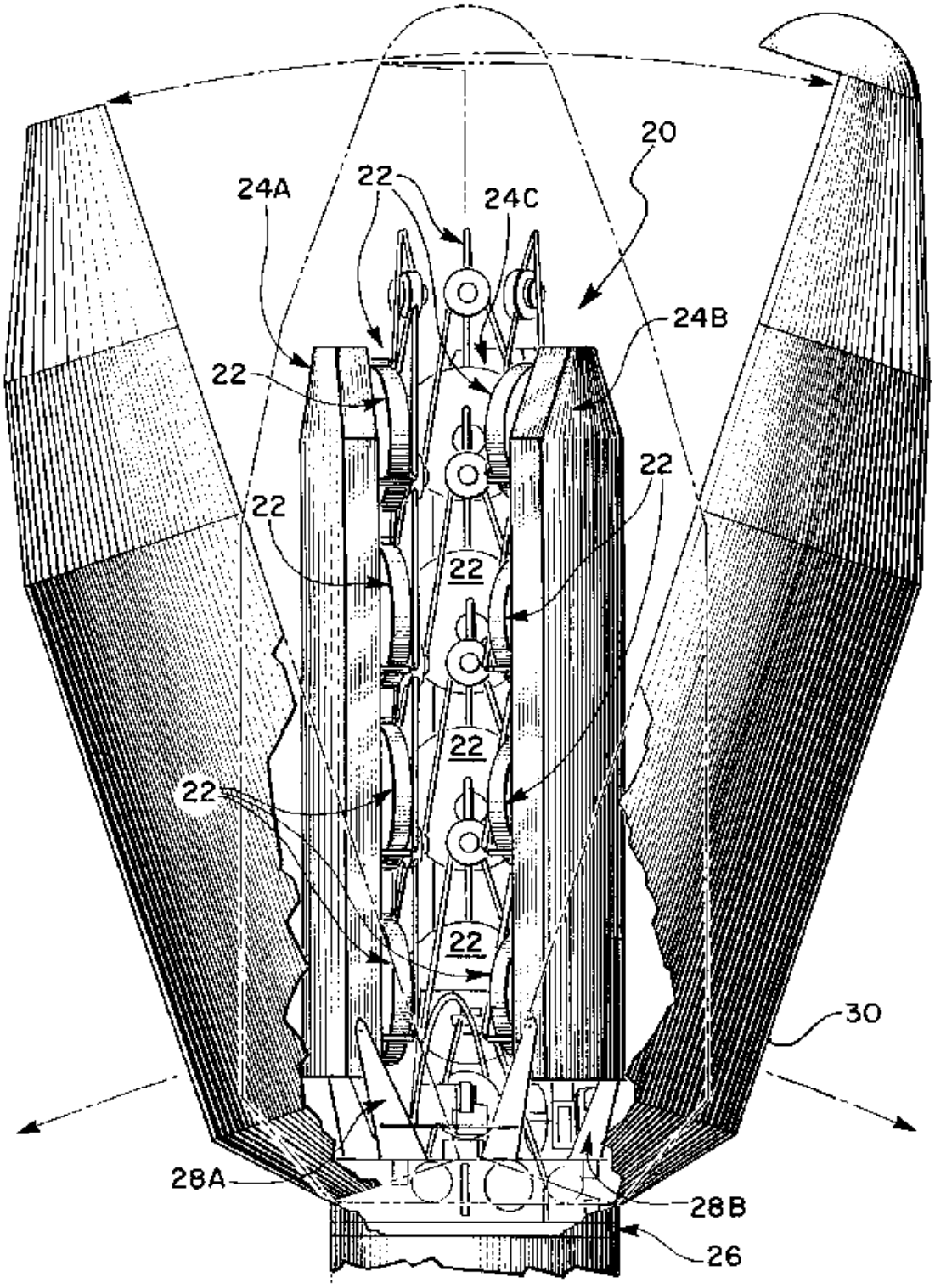

APPENDIX LL

Patent Design Pictures from Boeing Company [2]

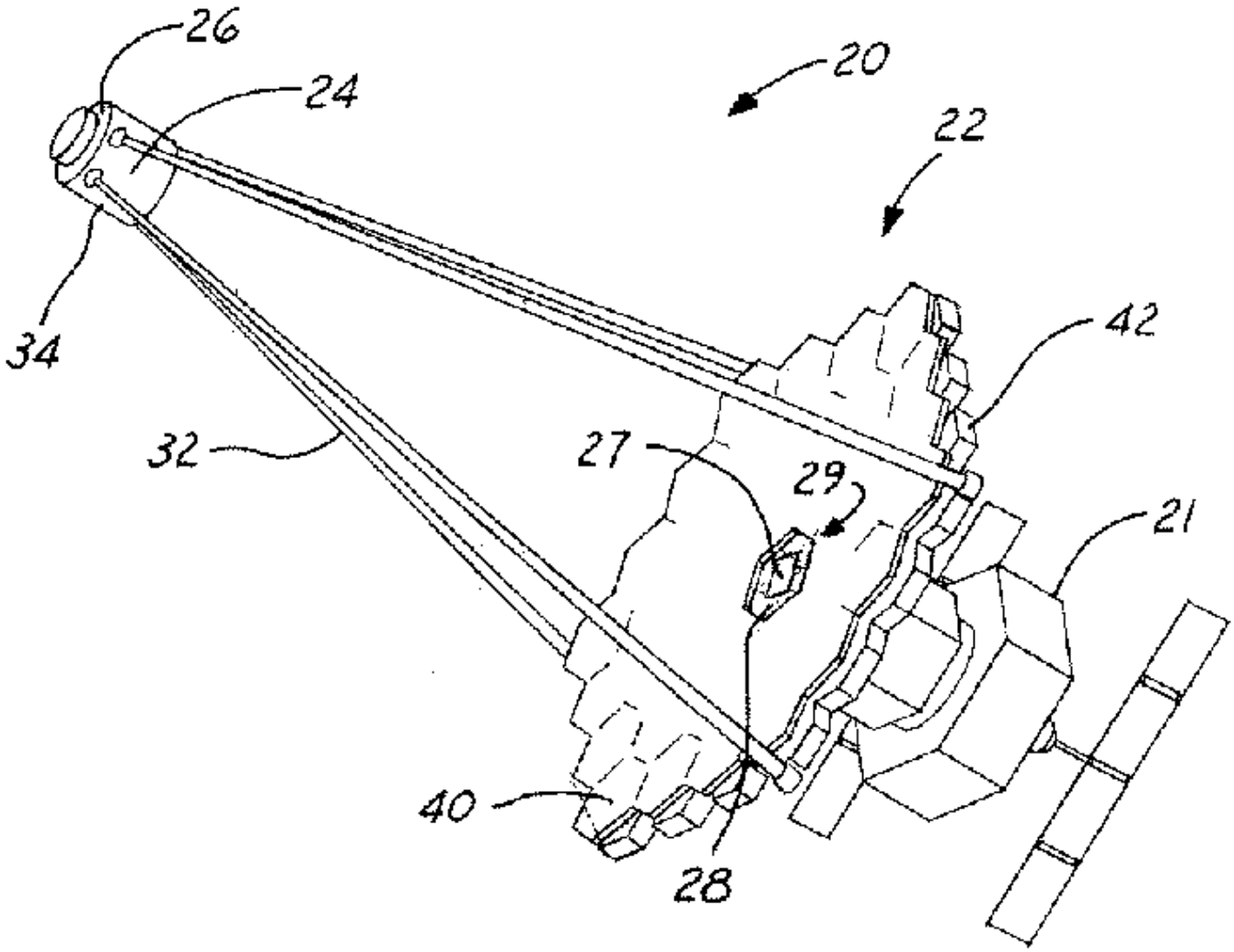

APPENDIX MM

Simulation results. Final model results are highlighted in gold.

G Direction (degrees from Y axis)	Shell Thickness (in)	Mesh Size (in)	Temp Load (Celsius)	Lattice Type	Mass (lb)	Modal Frequency (Hz)	Max Stress G + Temp (psi)	Lambda	Pass (Y/N)
0 degrees	0.15	0.2	35	TriDiametral	18.94	197.14	23640.00	40.67	Y
0 degrees	0.05	0.2	35	TriDiametral	7.91		47080.00	30.76	?
0 degrees	0.15	0.2	35	BiTriangle	19.22		24240.00	46.47	?
0 degrees	0.05	0.2	35	BiTriangle	7.18	127.46	48670.00	39.85	Y
0 degrees	0.15	0.2	35	QuadDiametral	19.33		16980.00	46.66	?
60 degrees	0.05	0.2	35	BiTriangle	7.18	127.46	45660.00	40.16	Y
60 degrees	0.08	0.2	35	BiTriangle	10.792		31960.00	42.63	?
0 degrees	0.05	0.2	35	QuadDiametral	7.29	130.44	34050.00	41.2	Y
0 degrees	0.05	0.2	35	QuadDiametral	7.29	130.44	33820.00	41.65	Y
0 degrees	0.05	0.2	35	TriDiametral	6.914	121.40	47080.00	30.76	Y
0 degrees	0.05	0.2	35	BiTriangle	7.18	127.46	48670.00	39.85	Y
60 degrees	0.05	0.2	35	QuadDiametral	7.29	130.44	33820.00	41.65	Y
0 degrees	0.05	0.2	35	QuadDiametral	7.29	130.44	34050.00	41.2	Y
0 degrees (towards leg)	0.05	0.2	35	QuadDiametral	8.419	124.05	18430.00	36.29	Y
0 degrees	0.05	0.05	35	QuadDiametral	8.47	Memory Error	30240.00	30.75	Y
180 degrees (between legs)	0.05	0.2	35	QuadDiametral	8.419	124.05	20890.00	36.65	Y
0 degrees	0.05	0.2	5	QuadDiametral	8.419	124.05	19120.00	36.30	Y